Time-dependent statistical properties of the electric microfield seen by a neutral radiator

Angel Alastuey*
Laboratoire de Physique Théorique et Hautes Energies, Université de Paris XI, 91405 Orsay, France

Joel L. Lebowitz
Department of Mathematics, Rutgers University, New Brunswick, New Jersey 08903

Dominique Levesque
Laboratoire de Physique Thérique et Hautes Energies, Université de Paris XI, 91405 Orsay, France
(Received 13 August 1990)

We study the dynamical properties of the electric microfield at a fixed neutral point immersed in a one-component plasma. We introduce an effective-field approach for describing the correlations between the microfield densities at two different times. In this approach, the essential features of the dynamics of the charges that produce the microfield are incorporated via suitable choices of the effective field. We present two versions of the theory which, in the static limits, reduce to the mean-force and adjustable-parameter exponential (APEX) approximations for the equilibrium distribution of the microfield. Both versions rely on a few ingredients determined through existent theories for the dynamics and the statics of the particles. The comparison to the molecular-dynamics data shows that the dynamical extension of APEX is the most reliable theory. The predictions of the Brissaud and Frisch model [J. Quant. Spectrosc. Radiat. Transfer **11**, 1767 (1971)] for the microfield dynamics are also tested against the simulation results. This model turns out to be rather reasonable. However, it is not as accurate as APEX, and it misses oscillatory behaviors (originating from the plasmon modes) which, on the contrary, are qualitatively reproduced by the latter theory.

I. INTRODUCTION

The statistical properties of the time-dependent electric microfield $\mathcal{E}(t)$ seen by a radiator (atom or ion) immersed in a plasma play a key role in the determination of the spectral line shapes.[1] In principle, all the correlations involving an arbitrary number of values of the microfield at different times are necessary for a complete description of the broadening and shifting mechanisms. Brissaud and Frisch[2] proposed a model for the time evolution of $\mathcal{E}(t)$, making the assumption that $\mathcal{E}(t)$ is a stationary Markov process. The central quantity is then the joint probability $P(\mathbf{E}t|\mathbf{E}_0 0)d\mathbf{E}\,d\mathbf{E}_0$ for $\mathcal{E}(t)$ to be in $d\mathbf{E}$ and for $\mathcal{E}(0)$ to be in $d\mathbf{E}_0$. This is specified via a Fokker-Planck equation that determines $P(\mathbf{E}t|\mathbf{E}_0 0)$ in terms of the static distribution $W(\mathbf{E})$ and of the autocorrelation function $\Gamma(t)=\langle \mathcal{E}(t)\cdot\mathcal{E}(0)\rangle$.

The Brissaud and Frisch model for Stark broadening is particularly attractive for the following reasons. First, it relies on ingredients which are reasonably known: $\Gamma(t)$ can be computed from plasma kinetic theory,[3] and there has been a large amount of theoretical work[4] dedicated to the determination of $W(\mathbf{E})$. Second, it allows a simple and unified calculation of the entire line shapes. Finally, the resulting profiles have high-frequency wings that reduced to those computed from the quasistatic approximation,[5,1] and their cores include effects which go beyond the impact approximation. Consequently, this model has been widely used in the calculations of atomic lines. It gives quite accurate results for electron broadening[6] (which is reasonably described by impact theories) and greatly improved results (compared with other theories) in the description of ion broadening.[7] Nevertheless, there are still important discrepancies with experimental data for ion broadening,[8] especially when the motion of the ions cannot be treated as a small perturbation (in general, the ions are assumed to be static during the relevant radiation times).

The discrepancies between the above model and the experimental data can be of various origins which will not be discussed here. However, as already noted by Smith, Talin, and Cooper,[8] the Markovian description of $P(\mathbf{E}t|\mathbf{E}_0 0)$ is rather crude, and is surely responsible for at least part of the discrepancies. The main purpose of this paper is to formulate an alternative approximation scheme for the joint probability density $P(\mathbf{E}t|\mathbf{E}_0 0)$, by explicitly taking into account that $\mathcal{E}(t)$ is the sum of the electric fields created by the charges of the plasma. This suggests an effective-field approach, in which the dynamics of the microfield is directly related to the motion of the plasma particles on the basis of reasonable physical arguments, without making an unfounded mathematical assumption about the nature of the process. The effective-field method provides simple and tractable representations of $P(\mathbf{E}t|\mathbf{E}_0 0)$ which should be useful in the calculations of line shapes.

The effective-field method which we present here extends to the dynamical case an approach[9] used previously for the derivation of approximate forms of the static distribution of the microfield.[10,11] It gives a generic approxi-

mate representation of $P(\mathbf{E}t|\mathbf{E}_0 0)$ in terms of a time-dependent effective-field $\mathbf{e}_t^*(\mathbf{r})$. As in the static case, the method allows various choices for $\mathbf{e}_t^*(\mathbf{r})$. We propose essentially two determinations of the latter, which reduce to their mean-force[11] and adjustable-parameter exponential[10] (APEX) approximations static counterparts respectively at $t=0$. The mean-force choice is inspired by a natural systematic expansion, while the APEX-like one is motivated by the very accurate description of $W(\mathbf{E})$ by APEX (including, in particular, the regime where the plasma particles are strongly correlated). The resulting effective-field expressions for $P(\mathbf{E}t|\mathbf{E}_0 0)$ incorporate the basic mechanisms which govern the statistics and the dynamics of the charges, e.g., the screening effects and the collective plasma oscillations. Moreover, their ingredients can be expressed in terms of well-known static quantities involving the particles.

As far as an accurate calculation of the whole spectral lines is concerned, it is necessary (and sometimes also sufficient[8]) that the approximate forms of $P(\mathbf{E}t|\mathbf{E}_0 0)$ accurately describe the statics, in the zero- and infinite-time limits, and the autocorrelation function $\Gamma(t)$, through their covariances. Here these conditions will be used for determining the best effective fields $\mathbf{e}_t^*(\mathbf{r})$. In this context, $\Gamma(t)$ takes on special importance. This motivated a detailed study[12] in this paper: we compute its short-time expansion and investigate the behavior of the probability distribution $P_t(\xi)$ of $\mathcal{E}(t)\cdot\mathcal{E}(0)$. In the same spirit, the equilibrium distribution of the time derivative of the microfield, $G(\mathbf{f})$, is another reduced dynamical quantity of interest whose determination does not require the full knowledge of $P(\mathbf{E}t|\mathbf{E}_0 0)$. While $\Gamma(t)$ is the crucial ingredient of the impact approximation[1] valid for fast moving charges, $G(\mathbf{f})$ is an important object in opposite situations where short-time expansions around the quasistatic approximation can be used.[13] Here, we derive a specific approximation for $G(\mathbf{f})$ which is independent of the effective-field theory of $P(\mathbf{E}t|\mathbf{E}_0 0)$. In addition to its own interest, the corresponding form of $G(\mathbf{f})$ might be used for imposing an additional constraint on the choice of the best effective-field $\mathbf{e}_t^*(\mathbf{r})$.

For the sake of simplicity, our calculations are restricted to the model one-component plasma (OCP). The OCP is a system of identical point charges immersed in a neutralizing rigid background. Here $\mathcal{E}(t)$ is the total electric field created at a fixed neutral point by the mobile charges and the background. This model is a good prototype for mimicking the statistical properties of the electric microfield seen by a radiating neutral atom immersed in a mixture of ions and electrons when the latter are strongly degenerate.

The paper is arranged as follows. In Sec. II, we define the model as well as the quantities of interest. Their relationships and some exact results are also established; in particular, the short-time expansion of $\langle \mathcal{E}(t)\cdot\mathcal{E}(0)\rangle$ (which diverges at $t=0$) is given up to the quadratic term. The general effective-field theory for $P(\mathbf{E}t|\mathbf{E}_0 0)$ is described in Sec. III, where the mean-force and APEX choices of $\mathbf{e}_t^*(\mathbf{r})$ are presented and justified. The physical interpretation of the former is also briefly discussed. In Sec. IV, we present the molecular-dynamics (MD) calculations of the above quantities. These data are used for testing the accuracy of our approximate theories and of the Brissaud and Frisch model. Rather than comparing $P(\mathbf{E}t|\mathbf{E}_0 0)$ itself, we study its Fourier transform with respect to the fields which is more directly accessible by both the MD simulations and the effective-field approaches. The successes and deficiencies of the above approximations are summarized in Sec. V. We also make there some concluding comments and remarks which concern the effective-field approach and its usefulness for line-shape calculations.

II. DEFINITIONS AND GENERAL SETTING

A. Model

The model considered throughout this paper is the one-component plasma. The OCP is a system of identical point particles of charge e and mass m, embedded in a uniform rigid background of the opposite charge. For a finite system made of N particles in a box with volume Λ, the background charge density is chosen equal to $-e\rho$ where $\rho=N/\Lambda$ is the mean-particle density: this ensures overall neutrality. The total interaction potential of the system is then given by

$$V(\mathbf{r}_1,\ldots,\mathbf{r}_N)=\tfrac{1}{2}\sum_{i\,(\neq j)} v(|\mathbf{r}_i-\mathbf{r}_j|)-\sum_{i=1}^{N}\int_\Lambda d\mathbf{r}\,\rho v(|\mathbf{r}-\mathbf{r}_i|) +\tfrac{1}{2}\int_{\Lambda^2} d\mathbf{r}\,d\mathbf{r}'\rho^2 v(|\mathbf{r}-\mathbf{r}'|)\,, \tag{2.1}$$

where $\mathbf{r}_i$ is the spatial position of the ith particle, and

$$v(r)=e^2/r \tag{2.2}$$

is the Coulomb potential.

In the following, we shall be interested in statistical properties of the time-dependent electric microfield $\mathcal{E}(t)$ produced at a fixed neutral point (the origin, for instance) by all the mobile charges and the background, i.e.,

$$\mathcal{E}(t)=\sum_{j=1}^{N}\mathbf{e}(\mathbf{r}_j(t))+\mathcal{E}_B\,. \tag{2.3}$$

In (2.3), $\mathbf{r}_j(t)$ is the spatial position of the jth particle at time t [all the particles moving in the potential (2.1)] while $\mathbf{e}(\mathbf{r})$ and $\mathcal{E}_B$ are the electric fields at the origin created, respectively, by a particle located at $\mathbf{r}$,

$$\mathbf{e}(\mathbf{r})=-e\frac{\mathbf{r}}{\mathbf{r}^3} \tag{2.4}$$

and the background,

$$\mathcal{E}_B=e\int_\Lambda d\mathbf{r}\,\rho\frac{\mathbf{r}}{\mathbf{r}^3}\,. \tag{2.5}$$

We shall consider that the system is in thermal equilibrium at temperature T ($\beta=1/k_B T$). The quantities of interest will be computed in the thermodynamic limit, i.e., $N\to\infty$, $\Lambda\to\infty$ with $\rho=N/\Lambda$ kept fixed. We shall assume that the former are well defined in this limit.[14] For notational convenience, it will not be explicitly specified in the equations that the above limit must be taken.

B. Joint probability density $P(\mathbf{E}t|\mathbf{E}_0 0)$

It follows from the definition of $P(\mathbf{E}t|\mathbf{E}_0 0)$ given in the Introduction that

$$P(\mathbf{E}t|\mathbf{E}_0 0)=\langle \delta(\mathcal{E}(t)-\mathbf{E})\delta(\mathcal{E}(0)-\mathbf{E}_0)\rangle \ , \tag{2.6}$$

where $\langle\ \rangle$ means a thermal equilibrium average over all the initial positions and velocities of the particles. At $t=0$, $P(\mathbf{E}t|\mathbf{E}_0 0)$ reduces to

$$P(\mathbf{E}t|\mathbf{E}_0 0)=\delta(\mathbf{E}-\mathbf{E}_0)W(\mathbf{E}_0) \ , \tag{2.7}$$

where $W(\mathbf{E}_0)$ is the static distribution of the electric microfield,

$$W(\mathbf{E}_0)=\langle \delta(\mathcal{E}(0)-\mathbf{E}_0)\rangle \ . \tag{2.8}$$

When $t\to\infty$, the microfields $\mathcal{E}(t)$ and $\mathcal{E}(0)$ should become uncorrelated. This implies that

$$\lim_{t\to\infty} P(\mathbf{E}t|\mathbf{E}_0 0)=P(\mathbf{E}\infty|\mathbf{E}_0 0)=W(\mathbf{E})W(\mathbf{E}_0) \ . \tag{2.9}$$

It is useful to introduce the Fourier transform $A_t(\mathbf{K},\mathbf{Q})$ of $P(\mathbf{E}t|\mathbf{E}_0 0)$,

$$\begin{aligned} A_t(\mathbf{K},\mathbf{Q})&=\int d\mathbf{E}\,d\mathbf{E}_0 \exp(i\mathbf{K}\cdot\mathbf{E}+i\mathbf{Q}\cdot\mathbf{E}_0)P(\mathbf{E}t|\mathbf{E}_0 0)\\ &=\langle \exp[i\mathbf{K}\cdot\mathcal{E}(t)+i\mathbf{Q}\cdot\mathcal{E}(0)]\rangle \end{aligned} \tag{2.10}$$

[the last line of (2.10) follows from the definition (2.6)]. Using the time-reversal invariance of the classical equations of motion and the spatial symmetries, it is easy to see that $A_t(\mathbf{K},\mathbf{Q})$ is a real symmetric function of $\mathbf{K}$ and $\mathbf{Q}$. Similarly to (2.7) and (2.9), $A_t(\mathbf{K},\mathbf{Q})$ can at $t=0$ and $t=\infty$ be expressed in terms of equilibrium static quantities. More precisely, one has

$$A_0(\mathbf{K},\mathbf{Q})=T(\mathbf{K}+\mathbf{Q}) \tag{2.11}$$

and

$$A_\infty(\mathbf{K},\mathbf{Q})=T(\mathbf{K})T(\mathbf{Q}) \ , \tag{2.12}$$

where $T(\mathbf{K})$ is the Fourier transform of $W(\mathbf{E})$,

$$\begin{aligned} T(\mathbf{K})&=\int d\mathbf{E}\exp(i\mathbf{K}\cdot\mathbf{E})W(\mathbf{E})\\ &=\langle \exp[i\mathbf{K}\cdot\mathcal{E}(0)]\rangle \ . \end{aligned} \tag{2.13}$$

Because of the rotation invariance of the infinite system, one has $T(\mathbf{K})=T(K)$ and $W(\mathbf{E})=W(E)$, while $A_t(\mathbf{K},\mathbf{Q})$ and $P(\mathbf{E}t|\mathbf{E}_0 0)$ only depend on the modulus of the vectors involved and on their relative angles.

C. Reduced dynamical quantities

The autocorrelation function of the electric microfield,

$$\Gamma(t)=\langle \mathcal{E}(t)\cdot\mathcal{E}(0)\rangle \ , \tag{2.14}$$

is just the covariance of $P(\mathbf{E}t|\mathbf{E}_0 0)$, i.e.,

$$\Gamma(t)=\int d\mathbf{E}\,d\mathbf{E}_0 \mathbf{E}\cdot\mathbf{E}_0 P(\mathbf{E}t|\mathbf{E}_0) \ . \tag{2.15}$$

On the other hand, using the expression (2.3) of the microfields in the definition (2.14), one can express $\Gamma(t)$ in terms of the time-displaced correlation functions of the particles with the result[3]

$$\Gamma(t)=8e^2\rho\int_0^\infty dk\ \tilde{S}(k,t) \ . \tag{2.16}$$

In (2.16), $\tilde{S}(k,t)$ is the usual dynamical structure factor defined by

$$\rho\tilde{S}(k,t)=\int d\mathbf{r}\exp(i\mathbf{k}\cdot\mathbf{r})\left\langle\left[\sum_{j=1}^{N}\delta(\mathbf{r}_j(t)-\mathbf{r})-\rho\right]\left[\sum_{i=1}^{N}\delta(\mathbf{r}_i(0)-\mathbf{0})-\rho\right]\right\rangle \ . \tag{2.17}$$

When $t\to\infty$, $\Gamma(t)$ goes to zero while for $t\to 0+$, $\Gamma(t)$ diverges because the covariance $\langle[\mathcal{E}(0)]^2\rangle$ of the static distribution $W(\mathbf{E})$ is infinite. The small-time behavior of $\Gamma(t)$ is studied in Appendix A. We find the following short-time expansion for $t>0$:

$$\frac{\Gamma(t)}{4(2\pi)^{1/2}e^2\rho\kappa_D}=\frac{1}{\omega_p t}+\left[\frac{2\pi}{3}\right]^{1/2}\frac{u_{\rm exc}(\Gamma)}{\Gamma^{3/2}}+\frac{\omega_p t}{72}+O(t^3) \ , \tag{2.18}$$

where $\kappa_D=(4\pi\rho\beta e^2)^{1/2}$ is the Debye wave number, $\omega_p=(4\pi\rho e^2/m)^{1/2}$ is the plasma frequency, $\Gamma=\beta e^2/a$ ($a=[3/(4\pi\rho)]^{1/3}$) is the coupling constant, and $u_{\rm exc}(\Gamma)$ is the excess internal energy per particle in units of $k_B T$ of the OCP. In units of ω_p^{-1}, the singular term of (2.18) is independent of ρ or β. It arises entirely from free motion and corresponds to the exact expression for $\Gamma(t)$ at all times for "free" particles.[15] The constant term in (2.18) depends on the thermodynamic state of the plasma which is characterized by the coupling constant Γ. The linear term which again depends only on ω_p is due to the interactions. There is no quadratic term.

The probability distribution of $\mathcal{E}(t)\cdot\mathcal{E}(0)$ is

$$P_t(\xi)=\langle \delta(\xi-\mathcal{E}(t)\cdot\mathcal{E}(0))\rangle \ , \tag{2.19}$$

which can be rewritten as

$$P_t(\xi)=\int d\mathbf{E}\,d\mathbf{E}_0\delta(\xi-\mathbf{E}\cdot\mathbf{E}_0)P(\mathbf{E}t|\mathbf{E}_0 0) \ . \tag{2.20}$$

At $t=0$ and $t=\infty$, $P_t(\xi)$ can be expressed entirely in terms of $W(E)$. Using successively (2.7) and (2.9) in (2.20), as well as the rotation invariance of the homogeneous infinite system, we obtain

$$P_0(\xi)=\begin{cases} 0, & \xi\le 0\\ \dfrac{1}{2\xi^{1/2}}P(\xi^{1/2}) \ , & 0<\xi \end{cases} \tag{2.21}$$

and

$$P_\infty(\xi)=\int_0^\infty dE\frac{1}{E}P(E)W_x\left[\frac{\xi}{E}\right], \tag{2.22}$$

where $P(E)$ is the probability distribution of the modulus of the field, $P(E)=4\pi E^2 W(E)$, and W_x is the probability distribution of one Cartesian component of the field.

Finally, we introduce the probability distribution of the time derivative of the electric microfield,

$$G(f)=\left\langle \delta\left[\mathbf{f}-\frac{d\mathcal{E}}{dt}\right]\right\rangle . \tag{2.23}$$

Because of the invariance of the equilibrium state under time evolution, $G(f)$ does not depend on the time. Its Fourier transform is given by

$$H(l)=\int d\mathbf{f}\exp(il\cdot\mathbf{f})G(f)$$
$$=\left\langle \exp\left[il\cdot\frac{d\mathcal{E}}{dt}(0)\right]\right\rangle . \tag{2.24}$$

Inserting $d\mathcal{E}/dt(0)=\lim_{t\to 0}\{[\mathcal{E}(t)-\mathcal{E}(0)]/t\}$ in (2.24), we immediately obtain

$$H(l)=\lim_{t\to 0}A_t\left[\frac{l}{t},-\frac{l}{t}\right] . \tag{2.25}$$

Furthermore, the calculation of $d\mathcal{E}/dt$ from (2.3) also gives

$$H(l)=\left\langle \exp\left[il\cdot\sum_{j=1}^N(\mathbf{v}_j\cdot\nabla_j)\mathbf{e}(\mathbf{r}_j)\right]\right\rangle$$
$$=\left\langle \exp\left[-\frac{1}{2m\beta}\sum_{j=1}^N[\nabla_j(l\cdot\mathbf{e}(\mathbf{r}_j))]^2\right]\right\rangle . \tag{2.26}$$

In deriving (2.26), we have used the fact that the velocity-dependent part of the equilibrium Gibbs measure is the product of the Gaussian factors $\exp(-\beta m v_j^2/2)$.

III. APPROXIMATE THEORIES

In this section, we formulate an effective-field approach of the time-dependent joint probability, which is a dynamical generalization of a similar method applied to the equilibrium distribution of the microfield. As in the static case, the general approach leads to various approximate theories according to the different possible choices of the effective field.

A. The effective-field approach

Our starting point is based on the coupling-parameter integration technique, first introduced in static microfield calculations by Iglesias.[9] Using (2.10), we find for fixed unit vectors $\hat{\mathbf{K}}$ and $\hat{\mathbf{Q}}$

$$\frac{\partial A_t}{\partial K}(\mathbf{K},\mathbf{Q})=\langle i\hat{\mathbf{K}}\cdot\mathcal{E}(t)\exp[i\mathbf{K}\cdot\mathcal{E}(t)+i\mathbf{Q}\cdot\mathcal{E}(0)]\rangle , \tag{3.1a}$$

$$\frac{\partial A_t}{\partial Q}(\mathbf{K},\mathbf{Q})=\langle i\hat{\mathbf{Q}}\cdot\mathcal{E}(0)\exp[i\mathbf{K}\cdot\mathcal{E}(t)+i\mathbf{Q}\cdot\xi(0)]\rangle . \tag{3.1b}$$

Dividing both sides of (3.1a) and (3.1b) by $A_t(\mathbf{K},\mathbf{Q})$ gives

$$\frac{\partial}{\partial K}\ln A_t(\mathbf{K},\mathbf{Q})=i\langle\hat{\mathbf{K}}\cdot\mathcal{E}(t)\rangle_{\mathbf{K},\mathbf{Q}} , \tag{3.2a}$$

$$\frac{\partial}{\partial Q}\ln A_t(\mathbf{K},\mathbf{Q})=i\langle\hat{\mathbf{Q}}\cdot\mathcal{E}(0)\rangle_{\mathbf{K},\mathbf{Q}} , \tag{3.2b}$$

where the measure which defines the average $\langle\ \rangle_{\mathbf{K},\mathbf{Q}}$ is the usual equilibrium Gibbs measure $d\mu_G$ multiplied by

$$\frac{\exp[i\mathbf{K}\cdot\mathcal{E}(t)+i\mathbf{Q}\cdot\mathcal{E}(0)]}{\langle\exp[i\mathbf{K}\cdot\mathcal{E}(t)+i\mathbf{Q}\cdot\mathcal{E}(0)]\rangle} .$$

Writing Eq. (3.2a) for the couple $(\mathbf{K}',\mathbf{Q})$ with $\mathbf{K}'=K'\hat{\mathbf{K}}$, and integrating the resulting equation from 0 to K, we obtain

$$\ln A_t(\mathbf{K},\mathbf{Q})=\ln T(Q)+i\int_0^K dK'\langle\hat{\mathbf{K}}\cdot\mathcal{E}(t)\rangle_{\mathbf{K}',\mathbf{Q}} . \tag{3.3a}$$

In deriving (3.3a), we have used $A_t(\mathbf{0},\mathbf{Q})=T(Q)$, which follows directly from the definitions (2.10) and (2.13). A similar manipulation of Eq. (3.2b) yields

$$\ln A_t(\mathbf{K},\mathbf{Q})=\ln T(K)+i\int_0^Q dQ'\langle\hat{\mathbf{Q}}\cdot\mathcal{E}(0)\rangle_{\mathbf{K},\mathbf{Q}'} . \tag{3.3b}$$

Since the electric microfield is a sum of one-body terms, the averages $\langle\ \rangle_{\mathbf{K}',\mathbf{Q}}$ and $\langle\ \rangle_{\mathbf{K},\mathbf{Q}'}$ appearing in (3.3a), and (3.3b) can be expressed in terms of generalized one-body densities. Using (2.3) we find

$$\langle\hat{\mathbf{K}}\cdot\mathcal{E}(t)\rangle_{\mathbf{K}',\mathbf{Q}}=\int d\mathbf{r}[\hat{\mathbf{K}}\cdot\mathbf{e}(\mathbf{r})][\rho_t^>(\mathbf{r}|\mathbf{K}',\mathbf{Q})-\rho] , \tag{3.4a}$$

$$\langle\hat{\mathbf{Q}}\cdot\mathcal{E}(0)\rangle_{\mathbf{K},\mathbf{Q}'}=\int d\mathbf{r}[\hat{\mathbf{Q}}\cdot\mathbf{e}(\mathbf{r})][\rho_t^<(\mathbf{r}|\mathbf{K},\mathbf{Q}')-\rho] , \tag{3.4b}$$

where the one-body densities $\rho_t^>$ and $\rho_t^<$ are

$$\rho_t^>(\mathbf{r}|\mathbf{K},\mathbf{Q})=\left\langle\sum_{j=1}^N\delta(\mathbf{r}_j(t)-\mathbf{r})\right\rangle_{\mathbf{K},\mathbf{Q}} , \tag{3.5a}$$

$$\rho_t^<(\mathbf{r}|\mathbf{K},\mathbf{Q})=\left\langle\sum_{j=1}^N\delta(\mathbf{r}_j(0)-\mathbf{r})\right\rangle_{\mathbf{K},\mathbf{Q}} . \tag{3.5b}$$

Note that

$$\rho_t^<(\mathbf{r}|\mathbf{K},\mathbf{Q})=\rho_t^>(\mathbf{r}|\mathbf{Q},\mathbf{K}) \tag{3.6}$$

as a consequence of the invariance properties of both the equations of motion and the equilibrium state. Using (3.4a) and (3.4b) in (3.3a) and (3.3b), respectively, and adding the resulting equations we finally obtain

$$A_t(\mathbf{K},\mathbf{Q})=\exp\left[\tfrac{1}{2}[F(K)+F(Q)]+\frac{i}{2}\int_0^K dK'\int d\mathbf{r}\,\hat{\mathbf{K}}\cdot\mathbf{e}(\mathbf{r})[\rho_t^>(\mathbf{r}|\mathbf{K}',\mathbf{Q})-\rho]+\frac{i}{2}\int_0^Q dQ'\int d\mathbf{r}\,\hat{\mathbf{Q}}\cdot\mathbf{e}(\mathbf{r})[\rho_t^<(\mathbf{r}|\mathbf{K},\mathbf{Q}')-\rho]\right] , \tag{3.7}$$

with

$$F(K)=\ln T(K) . \tag{3.8}$$

The expression (3.7) for $A_t(\mathbf{K},\mathbf{Q})$, which is formally exact, is the dynamical generalization of the following representation of $T(K)$:[9]

$$T(K)=\exp\left[i\int_0^K dK'\int d\mathbf{r}\,\hat{\mathbf{K}}\cdot\mathbf{e}(\mathbf{r})[\rho_{\mathbf{K}'}(\mathbf{r})-\rho]\right] . \tag{3.9}$$

In (3.9), $\rho_{\mathbf{K}'}(\mathbf{r})$ is the one-body density of the particles when the extra coupling $-i\mathbf{K}'\cdot\mathcal{E}(0)/\beta$ is added to the interaction potential V. In both (3.7) and (3.9), the $(-\rho)$ terms arise from the contributions of the background and ensure the absolute convergence of the spatial integrals. From now on, these terms can be omitted if we require that the angular integrations be performed first.

At this level, we have reduced the calculation of $A_t(\mathbf{K},\mathbf{Q})$ to the determination of the one-body densities $\rho_t^>$ and $\rho_t^<$. Although an exact evaluation of the latter quantities remain impossible, this reduction turns out to be quite useful for our purpose. Indeed, there exists a very simple prototype approximation for $\rho_t^>$ and $\rho_t^<$ which preserves the essential features of the dynamics of the microfield. This prototype approximation is a natural extension of the effective-field approximation for $\rho_{\mathbf{K}'}(\mathbf{r})$ which reads[16]

$$\rho_{\mathbf{K}'}(\mathbf{r})=\rho\exp[i\mathbf{K}'\cdot\mathbf{e}_0^*(\mathbf{r})] , \tag{3.10}$$

where $\mathbf{e}_0^*(\mathbf{r})$ is an effective field parallel to the bare Coulomb field $\mathbf{e}(\mathbf{r})$. Here we write

$$\rho_t^>(\mathbf{r}|\mathbf{K}',\mathbf{Q})=\rho\exp[i\mathbf{K}'\cdot\mathbf{e}_0^*(\mathbf{r})+i\mathbf{Q}\cdot\mathbf{e}_t^*(\mathbf{r})] , \tag{3.11a}$$

$$\rho_t^<(\mathbf{r}|\mathbf{K},\mathbf{Q}')=\rho\exp[i\mathbf{K}\cdot\mathbf{e}_t^*(\mathbf{r})+i\mathbf{Q}'\cdot\mathbf{e}_0^*(\mathbf{r})] , \tag{3.11b}$$

where $\mathbf{e}_t^*(\mathbf{r})$ is a time-dependent effective field which reduces to $\mathbf{e}_0^*(\mathbf{r})$ at $t=0$ and vanishes when $t\to\infty$ [note that (3.11a) and (3.11b) satisfy the exact relation (3.6)]. Using (3.10) in (3.9), and (3.11a) and (3.11b) in (3.7), we obtain

$$A_t^*(\mathbf{K},\mathbf{Q})=\exp\left[\tfrac{1}{2}\int d\mathbf{r}\,\rho\frac{\hat{\mathbf{K}}\cdot\mathbf{e}(\mathbf{r})}{\hat{\mathbf{K}}\cdot\mathbf{e}_0^*(\mathbf{r})}\{\exp[i\mathbf{K}\cdot\mathbf{e}_0^*(\mathbf{r})]-1\}\{\exp[i\mathbf{Q}\cdot\mathbf{e}_t^*(\mathbf{r})]+1\}\right.$$
$$\left.+\tfrac{1}{2}\int d\mathbf{r}\,\rho\frac{\hat{\mathbf{Q}}\cdot\mathbf{e}(\mathbf{r})}{\hat{\mathbf{Q}}\cdot\mathbf{e}_0^*(\mathbf{r})}\{\exp[i\mathbf{Q}\cdot\mathbf{e}_0^*(\mathbf{r})]-1\}\{\exp[i\mathbf{K}\cdot\mathbf{e}_t^*(\mathbf{r})]+1\}\right] . \tag{3.12}$$

The expression (3.12) is the required effective-field approximation for the Fourier transform (with respect to the fields) of the time-dependent conditional probability. It is easy to check that

$$A_0^*(\mathbf{K},\mathbf{Q})=T^*(|\mathbf{K}+\mathbf{Q}|) \tag{3.13}$$

and

$$A_\infty^*(\mathbf{K},\mathbf{Q})=T^*(K)T^*(Q) , \tag{3.14}$$

where $T^*(K)$ is the effective-field form of $T(K)$,

$$T^*(K)=\exp\left[\int d\mathbf{r}\,\rho\frac{\hat{\mathbf{K}}\cdot\mathbf{e}(\mathbf{r})}{\hat{\mathbf{K}}\cdot\mathbf{e}_0^*(\mathbf{r})}\{\exp[i\mathbf{K}\cdot\mathbf{e}_0^*(\mathbf{r})]-1\}\right] . \tag{3.15}$$

Equations (3.13) and (3.14) have the same structure as the exact equations (2.11) and (2.12). Therefore the effective-field approach does give the right limits at zero and infinite times, provided that the static distribution of the microfield is computed in the framework of this approximation. Aside from these requirements, the effective field $\mathbf{e}_t^*(\mathbf{r})$ is, up to now, rather arbitrary. In Sec. III B, we propose several reasonable reasonable choices of $\mathbf{e}_t^*(\mathbf{r})$, which take into account both the dynamics of the particles and the static properties.

B. Determination of the effective fields

1. *Mean-force approximation*

Our first choice of $\mathbf{e}_t^*(\mathbf{r})$ is inspired by a cumulantlike expansion of the generalized one-body densities $\rho_t^>$ and $\rho_t^<$. Indeed, the expression (3.5a) and (3.5b) can be rewritten as

$$\rho_t^>(\mathbf{r}|\mathbf{K},\mathbf{Q})=\rho\frac{\langle\exp[i\mathbf{K}\cdot\mathcal{E}(t)+i\mathbf{Q}\cdot\mathcal{E}(0)]\rangle_{\mathbf{r}}^>}{\langle\exp[i\mathbf{K}\cdot\mathcal{E}(t)+i\mathbf{Q}\cdot\mathcal{E}(0)]\rangle} , \tag{3.16a}$$

$$\rho_t^<(\mathbf{r}|\mathbf{K},\mathbf{Q})=\rho\frac{\langle\exp[i\mathbf{K}\cdot\mathcal{E}(t)+i\mathbf{Q}\cdot\mathcal{E}(0)]\rangle_{\mathbf{r}}^<}{\langle\exp[i\mathbf{K}\cdot\mathcal{E}(t)+i\mathbf{Q}\cdot\mathcal{E}(0)]\rangle} , \tag{3.16b}$$

where $\langle\ \rangle_{\mathbf{r}}^>$ and $\langle\ \rangle_{\mathbf{r}}^<$ denote averages with the measures

$$d\mu_G\sum_{j=1}^N\delta(\mathbf{r}_j(t)-\mathbf{r})/\rho$$

and

$$d\mu_G\sum_{j=1}^N\delta(\mathbf{r}_j(0)-\mathbf{r})/\rho ,$$

respectively. The cumulant expansions of both the numerators and the denominators of (3.16a) and (3.16b) give

$$\rho_t^>(\mathbf{r}|\mathbf{K},\mathbf{Q})=\rho\exp[i\mathbf{K}\cdot\langle\mathcal{E}(t)\rangle_{\mathbf{r}}^>+i\mathbf{Q}\cdot\langle\mathcal{E}(0)\rangle_{\mathbf{r}}^>+\cdots] , \tag{3.17a}$$

$$\rho_t^<(\mathbf{r}|\mathbf{K},\mathbf{Q})=\rho\exp[i\mathbf{K}\cdot\langle\mathcal{E}(t)\rangle_{\mathbf{r}}^<+i\mathbf{Q}\cdot\langle\mathcal{E}(0)\rangle_{\mathbf{r}}^<+\cdots] \tag{3.17b}$$

[the terms omitted in (3.17a) and (3.17b) are at least of second order with respect to **K** and **Q**]. Keeping only the first terms, linear in **K** and **Q**, in the above expansions, we obtain an approximate representation of $\rho_t^>$ and $\rho_t^<$ which is of the effective-field type (3.11) with

$$\mathbf{e}_t^*(\mathbf{r})=\mathbf{e}_t^{\mathrm{MF}}(\mathbf{r})=\langle \mathscr{E}(t)\rangle_{\mathbf{r}}^< =\langle \mathscr{E}(0)\rangle_{\mathbf{r}}^> =\int d\mathbf{r}' e(\mathbf{r}')S(|\mathbf{r}-\mathbf{r}'|,t)\ , \tag{3.18}$$

and where

$$S(|\mathbf{r}-\mathbf{r}'|,t)=\frac{1}{\rho}\left\langle \left[\sum_{j=1}^{N}\delta(\mathbf{r}_j(t)-\mathbf{r})-\rho\right]\left[\sum_{i=1}^{N}\delta(\mathbf{r}_i(0)-\mathbf{r}')-\rho\right]\right\rangle \tag{3.19}$$

is the truncated total Van Hove function of the particles [the dynamical structure factor $\tilde{S}(k,t)$ is nothing but the spatial Fourier transform of $S(r,t)$]. The expression (3.18) of $\mathbf{e}_t^*(\mathbf{r})$ appears as a natural extension of the mean-force field approximation[11] for the static effective field which reads [$S(r)\equiv S(r,t=0)$]

$$\mathbf{e}_0^{\mathrm{MF}}(\mathbf{r})=\int d\mathbf{r}'\mathbf{e}(\mathbf{r}')S(|\mathbf{r}'-\mathbf{r}|)\ . \tag{3.20}$$

Furthermore, let us emphasize that the corresponding approximate joint probability has the right covariance (2.16). This can be easily checked by calculating the coefficient of the $(\mathbf{K}\cdot\mathbf{Q})$ term in the expansion of $A_t^{\mathrm{MF}}(\mathbf{K},\mathbf{Q})$ at small **K** and **Q** [this coefficient, up to a minus sign, is equal to the covariance of $P^{\mathrm{MF}}(\mathbf{E}t|\mathbf{E}_0 0)$].

For practical purposes, it still remains to find a simple and accurate representation of $S(r,t)$. In fact, such a representation exists in the literature; it is known as the "three-pole" approximation.[17] The latter is based on the Mori continuous fraction expansion[18] of

$$\tilde{S}(k,\omega)=(2\pi)^{-1}\int_{-\infty}^{\infty}dt\,\exp(i\omega t)\tilde{S}(k,t)\ ,$$

which is truncated at the third order. The corresponding rational fraction in ω, $\tilde{S}_{3P}(k,\omega)$, has the right second and fourth moments (which are expressible in terms of static quantities), and has three pairs of complex-conjugate poles in the complex plane. The Fourier transform of the former with respect to ω gives (see Appendix B)

$$\tilde{S}_{3P}(k,t)=\frac{2\omega_0^2\delta}{\alpha^2+(\gamma-\delta)^2}\left[\frac{\exp(-\gamma t)}{\gamma}+\frac{\exp(-\delta t)}{2\alpha\delta(\alpha^2+\delta^2)}\mathrm{Re}\{(\alpha-i\delta)[\alpha+i(\gamma-\delta)][\alpha-i(\gamma+\delta)]\exp(i\alpha t)\}\right]\ . \tag{3.21}$$

In (3.21) one has

$$\omega_0^2=\frac{k^2}{m\beta}\ , \tag{3.22a}$$

while α, γ, and δ can be expressed in terms of the frequencies ω_{0l} and ω_{1l} and of the relaxation time τ_{3P} defined through

$$\omega_{0l}^2=\frac{k^2}{m\beta\tilde{S}(k)}\ , \tag{3.22b}$$

$$\omega_{1l}^2=\omega_p^2\left[1+\frac{3k^2}{\kappa_D^2}-2\int_0^{\infty}dr\frac{1}{r}\left[\frac{\sin(kr)}{kr}+\frac{3\cos(kr)}{(kr)^2}-\frac{3\sin(kr)}{(kr)^3}\right]h(r)\right]\ , \tag{3.22c}$$

$$\tau_{3P}=\frac{\pi^{1/2}}{2}\frac{1}{(\omega_{1l}^2-\omega_{0l}^2)^{1/2}}\ , \tag{3.22d}$$

where $h(\mathbf{r})$ is the Ursell function [$S(r)=\delta(\mathbf{r})+\rho h(r)$]. One finds

$$\gamma=\frac{1}{3\tau_{3P}}+\left[\frac{(b^2+4c^3/27)^{1/2}-b}{2}\right]^{1/3}-\left[\frac{(b^2+4c^3/27)^{1/2}+b}{2}\right]^{1/3}\ , \tag{3.23}$$

with

$$b=\frac{\omega_{1l}^2-3\omega_{0l}^2}{3\tau_{3P}}-\frac{2}{27\tau_{3P}^3}\ , \tag{3.24a}$$

$$c=\omega_{1l}^2-\frac{1}{3\tau_{3P}^2}\ , \tag{3.24b}$$

and the expressions for δ and α are obtained by replacing (3.23) in

$$\delta=\frac{1}{2\tau_{3P}}-\frac{\gamma}{2} \tag{3.25}$$

and

$$\alpha=\left[\omega_{1l}^2+\frac{3\gamma^2}{4}-\frac{\gamma}{2\tau_{3P}}-\frac{1}{4\tau_{3P}^2}\right]^{1/2} . \tag{3.26}$$

As seen from Eqs. (3.21)–(3.26), the sole ingredient of the "three-pole" approximation is the static structure factor $\tilde{S}(k)$. In the following, we shall use the mean-force approximation for $P(\mathbf{E}t|\mathbf{E}_0 0)$ only for $\Gamma \leq 1$, because the corresponding description of the static limits at $t=0$ and $t=\infty$ becomes too bad in the intermediate coupling regime [even when accurate representations for $\tilde{S}(k)$ are used[19]]. It is then legitimate to replace $\tilde{S}(k)$ by its Debye-Hückel form which is asymptotically exact in the weak-coupling limit.

2. APEX-like approximation

A second choice is inspired by the APEX theory[10] of the static distribution $W(\mathbf{E})$. In the latter, the static effective field is assumed to have the form

$$\mathbf{e}_0^*(\mathbf{r})=\mathbf{e}_0^{\mathrm{AP}}(\mathbf{r})=\frac{-e}{r^2}(1+\kappa_A r)\exp(-\kappa_A r)\hat{\mathbf{r}} , \tag{3.27}$$

where κ_A is the APEX wave number,[11]

$$\kappa_A=-\frac{2u_{\mathrm{exc}}(\Gamma)}{3^{1/2}\Gamma^{3/2}}\kappa_D . \tag{3.28}$$

In order to determine a time-dependent effective field which reduces to the field (3.27) at $t=0$, we rewrite the latter as

$$\mathbf{e}_0^{\mathrm{AP}}(\mathbf{r})=\int d\mathbf{r}'\mathbf{e}(\mathbf{r}')D_A(|\mathbf{r}'-\mathbf{r}|) , \tag{3.29}$$

where the distribution $D_A(r)$ is such that

$$\int d\mathbf{r}\, D_A(r)\exp(i\mathbf{k}\cdot\mathbf{r})=\tilde{D}_A(k)=\frac{k^2}{k^2+\kappa_A^2} . \tag{3.30}$$

We now make the *ad hoc* assumption

$$\mathbf{e}_t^*(\mathbf{r})=\mathbf{e}_t^{\mathrm{AP}}(\mathbf{r})=\int d\mathbf{r}'\mathbf{e}(\mathbf{r}')D_A(|\mathbf{r}'-\mathbf{r}|,t) , \tag{3.31}$$

where the Fourier transform

$$\tilde{D}_A(k,t)=\int d\mathbf{r}\exp(i\mathbf{k}\cdot\mathbf{r})D_A(r,t) \tag{3.32}$$

is given by

$$\tilde{D}_A(k,t)=B_A(k)\exp\left[-\frac{t}{\tau_A(k)}\right]+C_A(k)\exp\left[-\frac{t}{\tau_A(k)}\right]\cos[\omega_A(k)t] . \tag{3.33}$$

The form (3.33) is inspired from both the three-pole and the hydrodynamical expressions[20] of $\tilde{S}(k,t)$. The amplitude coefficients $B_A(k)$ and $C_A(k)$, as well as the relaxation time $\tau_A(k)$ and the frequency $\omega_A(k)$, are determined through the following requirements. First, one has the zero-time constraint

$$B_A(k)+C_A(k)=\frac{k^2}{k^2+\kappa_A^2} , \tag{3.34}$$

which ensures that $\mathbf{e}_t^{\mathrm{AP}}(\mathbf{r})$ does reduce to (3.27) at $t=0$. Second, we impose that

$$\tilde{D}_A(k,t)\sim\frac{k^2}{\kappa_A^2}\cos(\omega_p t), \quad k\to 0 . \tag{3.35}$$

This behavior is similar to the exact behavior of $\tilde{S}(k,t)$ (Ref. 21) (apart from the replacement of κ_D by κ_A); it incorporates the fact that the dynamics for long wavelengths are governed by the undamped plasmon oscillations at the plasma frequency ω_p.[22] Third, the frequency $\omega_A(k)$ is such that

$$\frac{1}{\omega_A}\frac{d\omega_A}{dk}=\frac{\chi_T^0}{\chi_T}\frac{a}{3\Gamma} \tag{3.36}$$

at $k=0$, where χ_T^0/χ_T is the ratio of the isothermal compressibilities of an ideal gas and of the OCP. This takes into account the main features of the plasmon dispersion relation $\omega_{\mathrm{plasmon}}(k)$, since the right-hand side (rhs) of (3.36) is the average over $[0,2/a]$ of a simplified version of a phenomenological hydrodynamic expression[23] of $[d\omega_{\mathrm{plasmon}}(k)/dk]/\omega_p$ (the notion of plasmon mode does not make sense[22] for $ka\geq 2$). Finally, we optimize the autocorrelation function

$$\Gamma^{\mathrm{AP}}(t)=\rho\int d\mathbf{r}\,\mathbf{e}(\mathbf{r})\cdot\mathbf{e}_t^{\mathrm{AP}}(\mathbf{r})=8e^2\rho\int_0^\infty dk\,\tilde{D}_A(k,t) \tag{3.37}$$

by reproducing the exact short-time expansion (2.18) of $\Gamma(t)$, up to the constant term included. The above requirements are satisfied by the simple functions

$$B_A(k)=\left[1-\exp\left[-\eta_A\frac{k^2}{\kappa_D^2}\right]\right]^2 , \tag{3.38a}$$

$$C_A(k)=\frac{k^2}{k^2+k_A^2}-\left[1-\exp\left[-\eta_A\frac{k^2}{\kappa_D^2}\right]\right]^2 , \tag{3.38b}$$

$$\tau_A(k)=\left[\frac{\pi}{2}\right]^{1/2}\frac{\kappa_D}{\omega_p k} , \tag{3.38c}$$

$$\omega_A(k)=\omega_p\left[1+\frac{1}{\sqrt{3\Gamma}}\frac{\chi_T^0}{\chi_T}\frac{k}{\kappa_D}\right] , \tag{3.38d}$$

where the dimensionless parameter η_A controls the first zero of $\Gamma^{\mathrm{AP}}(t)$ and will be determined later. Note that all the other ingredients of the present approximation only depend on static quantities, namely, u_{ex} and χ_T^0/χ_T, which are rather well known.

C. Comments

The mean-force choice (3.18) for the effective field appears to be more natural than the APEX one (3.31) since it involves the dynamical structure factor of the particles. However, this does not guarantee that the corresponding mean-force theory is better than APEX, as illustrated by the static case where APEX is the more accurate approximation. In fact, the description of the dynamics of the microfield in terms of a finite number of time-displaced particle correlations obviously is incomplete. Conse-

quently, there is no fundamental need to define effective fields which incorporate in a precise way the above correlations. This justifies the introduction of APEX which, in addition to its simplicity, takes into account basic physical mechanisms such as screening effects and plasma oscillations.

In the static case, the effective-field theory has a simple interpretation. It amounts to introducing an auxiliary system of independent quasiparticles with density $\rho[e(\mathbf{r})/e_0^*(\mathbf{r})]$ and creating the field $\mathbf{e}_0^*(\mathbf{r})$. The effective-field form of the distribution of the electric microfield created by the plasma particles is then identical to the Holtsmark distribution of the field created by the quasiparticles [see Eq. (3.15)]. In the present dynamical case, such an interpretation no longer holds. In other words, the effective-field expression (3.12) cannot be identified with the distribution of any auxiliary system of independent quasiparticles. This is due to the fact that the effective-field approach incorporates essential features of the dynamics of the particles (like the collision processes) which are not reducible to the trivial dynamics of independent quasiparticles moving on straight lines.

IV. COMPARISON OF THE APPROXIMATE THEORIES TO MD DATA

In this section we compare the predictions of various approximate theories, among which are the effective-field approaches derived in Sec. III, to the results of MD calculations. First, we briefly describe the method used in the MD simulations. Then, we turn to the results, considering successively the static quantities $T(K)$, $P_0(\xi)$, and $P_\infty(\xi)$, the reduced dynamical objects $\Gamma(t)$ and $H(l)$, and finally the full distribution $A_t(\mathbf{K},\mathbf{Q})$. Comparisons are restricted to the weak-coupling and intermediate coupling regimes ($\Gamma \leq 10$).

A. The MD method

The OCP has been studied by numerical simulation[24–26] and today its equilibrium and dynamical properties are known with very good precision. The details of the application of the MD method to the OCP are given in Ref. 24 and we summarize here only the main points of the procedures used for the numerical calculations of $A_t(\mathbf{K},\mathbf{Q})$, $\Gamma(t)$, etc.

In the present simulations, we have computed the trajectories of 256 ions enclosed in a cubic volume Λ. To take into account the periodic boundary conditions of Λ, the interaction between the ions was not the simple Coulomb potential but the "Ewald" Coulomb potential.[26] The electric field $\mathcal{E}(t)$ needed for the computation of $P(\mathbf{E}t|\mathbf{E}_0 0)$ or $A_t(\mathbf{K},\mathbf{Q})$ is the field at a neutral point $\mathbf{r}$ of Λ; from Eq. (2.3) this field is

$$\mathcal{E}(t)=\sum_{j=1}^{N}\mathbf{e}^{\omega}[\mathbf{r}_j(t)-\mathbf{r}]\ , \tag{4.1}$$

where $\mathbf{e}^{\omega}[\mathbf{r}_j(t)-\mathbf{r}]$ is the field due to the jth ion at the point $\mathbf{r}$ derived from the "Ewald" potential. In Λ all the points $\mathbf{r}$ are equivalent; we have calculated, at each integration step of the simulations, 1024 values of $\mathcal{E}(t)$ for 1024 different points $\mathbf{r}$. These points were located to the nodes of a bcc lattice inside Λ. This particular choice of points $\mathbf{r}$ was allowed because our simulations were made in the fluid phase of the OCP. The quantities $A_t(\mathbf{K},\mathbf{Q}), T(K), \Gamma(t), \ldots$ were estimated from averages over these values of $\mathcal{E}(t)$.

Three sets of MD runs were performed for Γ in the vicinity of 1, 5, and 10; for each value of Γ the cumulate number of integration steps of these runs was 20 000. At these temperatures this number was sufficient to estimate the dynamical and equilibrium quantities with an uncertainty of a few percent. For instance, the values of u_{ex} were -0.579, -3.743, and -7.989 for the precise values of $\Gamma=1.007$, 4.985, and 10.006.

B. Static quantities

The static functions $T(K)$, $P_0(\xi)$, and $P_\infty(\xi)$ evaluated by MD are presented in Figs. 1, 2, and 3, respectively. The decrease of $T(K)$ is faster for $\Gamma=1$ than for $\Gamma=5$ and $\Gamma=10$. The domain of K where the values of $T(K)$ are larger than the statistical noise is $K<5a^2/e$. The statistical error on this function is estimated of the order of 2%. The distribution $P_\infty(\xi)$ is obtained from the comparison between the MD data for $P_t(\xi)$ at successive large times. This comparison shows that $P_t(\xi)$ has reached its asymptotic value (with a precision of 1 or 2%) for $t\sim 2\tau_0$ at $\Gamma=1$, and for $t\sim 5\tau_0$ at $\Gamma=5,10$, where the relaxation time τ_0 is defined by

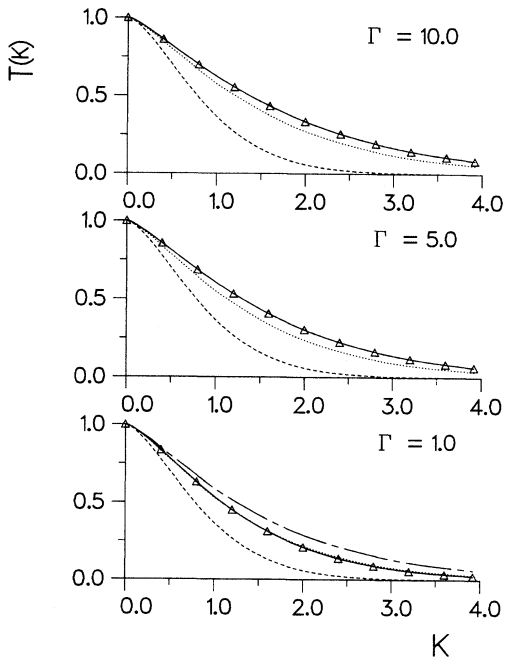

FIG. 1. The Fourier transform $T(K)$ of the probability distribution of the electric field at $\Gamma=1$, 5, and 10. K is in units of a^2/e. Solid line and triangles, MD; dotted line, APEX. Dashed line, Holtzmark; dash-dotted line, mean-force.

$$\tau_0=\left[\frac{ma^3}{e^2}\right]^{1/2}=\frac{\sqrt{3}}{\omega_p}\ . \tag{4.2}$$

The distributions $P_0(\xi)$ and $P_\infty(\xi)$ are rather broad. For instance, at $t=0$, the most probable value of ξ differs strongly from the average value.

The mean-force and APEX versions of the effective-field form (3.15) of $T(K)$ are obtained by replacing $\mathbf{e}_0^*(r)$ by $\mathbf{e}_0^{\mathrm{MF}}(\mathbf{r})$ and $\mathbf{e}_0^{\mathrm{AP}}(\mathbf{r})$, respectively. This gives

$$T^{\mathrm{MF,AP}}(K)=\exp\left[4\pi\rho e\int_0^\infty dr\frac{1}{e_0^{\mathrm{MF,AP}}(r)}\left[\frac{\sin[Ke_0^{\mathrm{MF,AP}}(r)]}{Ke_0^{\mathrm{MF,AP}}(r)}-1\right]\right], \tag{4.3}$$

where $e_0^{\mathrm{AP}}(r)$ is given by (3.27), while $e_0^{\mathrm{MF}}(r)$ has a similar expression with κ_D in place of κ_A. We recall that this expression of $e_0^{\mathrm{MF}}(r)$ amounts to replacing $S(|\mathbf{r}'-\mathbf{r}|)$ by its Debye-Hückel form in (3.20). The corresponding form of $T^{\mathrm{MF}}(K)$ is particularly simple, since it does not involve any ingredient which has to be determined by other theories. The sole ingredient of $T^{\mathrm{AP}}(K)$ is the ratio κ_A/κ_D which, according to (3.28), requires knowledge of $u_{\mathrm{exc}}(\Gamma)$. A sophisticated fit of the latter[27] gives

$$\kappa_A/\kappa_D=\begin{cases}0.660\\0.387\\0.292,\end{cases}\quad\Gamma=\begin{cases}1\\5\\10\ .\end{cases} \tag{4.4}$$

The curves representing $T^{\mathrm{MF}}(K)$ and $T^{\mathrm{AP}}(K)$ (with K in units of a^2/e) are shown in Fig. 1. At $\Gamma=1$, the agreement between APEX and the MD results is excellent, within statistical error. The mean-force approximation slightly overestimates the values of $T(K)$. This defect becomes very important at $\Gamma=5,10$ [even when a more accurate description of $S(|\mathbf{r}'-\mathbf{r}|)$ than Debye-Hückel is used[19]] and the corresponding curves are not shown. For these values of Γ, a significative disagreement between APEX and MD progressively appears for large K. However, the APEX predictions remain quite reasonable over a wide range of K.

The static distributions $W^{\mathrm{MF}}(E)$ and $W^{\mathrm{AP}}(E)$ are easily computed by taking (numerically) the three-dimensional inverse Fourier transform with respect to $\mathbf{K}$ of (4.3), i.e.,

$$W^{\mathrm{MF,AP}}(E)=\frac{1}{2\pi^2E}\int_0^\infty dK\,K\sin(KE)T^{\mathrm{MF,AP}}(K)\ . \tag{4.5}$$

Similarly, the corresponding distribution of a Cartesian component E_x of $\mathbf{E}$ is given by one-dimensional Fourier transform, i.e.,

$$W_x^{\mathrm{MF,AP}}(E_x)=\frac{1}{\pi}\int_0^\infty dK\cos(KE_x)T^{\mathrm{MF,AP}}(K)\ . \tag{4.6}$$

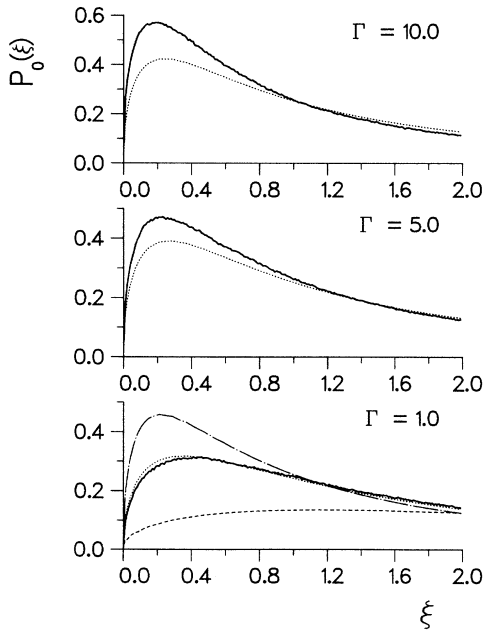

FIG. 2. The probability distribution $P_0(\xi)$ of $[\mathcal{E}(0)]^2$ at $\Gamma=1$, 5, and 10. ξ is in units of e^2/a^4. Solid line, MD; dotted line, APEX; dash-dotted line, mean-force; dashed line, Holtsmark. The mean-force and Holtsmark curves are not shown at $\Gamma=5$ and 10.

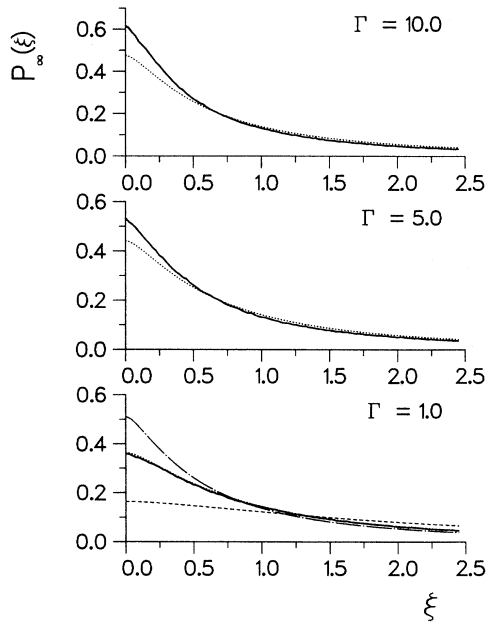

FIG. 3. The same as Fig. 2 for the probability distribution $P_\infty(\xi)$ of $\mathcal{E}(\infty)\cdot\mathcal{E}(0)$.

The distributions $P_0^{MF,AP}(\xi)$ and $P_\infty^{MF,AP}(\xi)$ are then calculated by inserting (4.5) and (4.6) into (2.21) and (2.22). The results are displayed in Figs. 2 and 3. At $\Gamma=1$, $P_0^{MF}(\xi)$ and $P_\infty^{MF}(\xi)$ are too large for small values of ξ, because the whole distribution $W^{MF}(E)$ is shifted to low fields with respect to the "exact" MD distribution. When ξ increases, the accuracy of the mean-force theory improves. As could be expected from the above study of $T(K)$, the accuracy of APEX over the full range of ξ is remarkable at $\Gamma=1$. At $\Gamma=5,10$, this accuracy becomes less spectacular, but the relative disagreements with the MD data do not exceed a few percent.

C. Reduced dynamical quantities

1. *The autocorrelation function of the field*

The function $\Gamma(t)$ has been calculated for the three values of Γ and the MD results are plotted in Figs. 4 and 5. The exact value of $\langle \mathcal{E}^2(0)\rangle$ is infinite due to the fact that during the evolution of the system at some values of t the position of an ion can coincide with any point of Λ. In the MD simulation, due to the finite duration of the runs and the limited number of points $\mathbf{r}$ used for the sampling of $\mathcal{E}(t)$, these events do not occur. This shortcoming of the MD simulation increases the statistical uncertainty on $\Gamma(t)$ at small time where rare but very large contributions are missing in the statistical averages. The comparison between the results of independent simulations at constant Γ and also with the exact small-time expansion (2.18) of $\Gamma(t)$ leads to the conclusion that the MD data for this function are not reliable for $t<0.2\tau_0$ and that the statistical error on $\Gamma(t)$ for $t\geq\tau_0$ is about 10–15%.

In principle, the mean-force effective-field theory should give the right covariance $\Gamma(t)$ of $P(\mathbf{E}t|\mathbf{E}_0 0)$, provided that the exact Van Hove function $S(|\mathbf{r}-\mathbf{r}'|,t)$ is used in (3.18). Here, the replacement of the latter by the "three-pole" form (3.21) leads to an approximate covariance,

$$\Gamma^{MF}(t)=\rho\int d\mathbf{r}\,\mathbf{e}(\mathbf{r})\cdot\mathbf{e}_t^{MF}(\mathbf{r}) = 8e^2\rho\int_0^\infty dk\,\tilde{S}_{3P}(k,t)\ . \tag{4.7}$$

At $\Gamma=1$, $\Gamma^{MF}(t)$ reproduces the oscillatory behavior of $\Gamma(t)$ (see Fig. 4). The amplitude of the negative first oscillation is well described, while the amplitude of the positive second oscillation is overestimated. Furthermore, there is a phase difference between the oscillations of $\Gamma^{MF}(t)$ and those of $\Gamma(t)$; in particular, the zeros of $\Gamma^{MF}(t)$ are shifted to smaller times with respect to the MD ones. These shortcomings of $\Gamma^{MF}(t)$ are due mainly to the "three-pole" approximation itself, rather than to the use of the Debye-Hückel form for $\tilde{S}(k)$ [we have checked that the replacement of $\tilde{S}(k)$ by its hypernetted-chain (HNC) expression does not modify significantly $\Gamma^{MF}(t)$].

In the APEX effective-field approach, the function $\Gamma(t)$ plays the role of an ingredient, which is used as a constraint for choosing $\mathbf{e}_t^{AP}(\mathbf{r})$. In particular, the expression (3.31) of $\mathbf{e}_t^{AP}(\mathbf{r})$ together with (3.33) and (3.38) gives

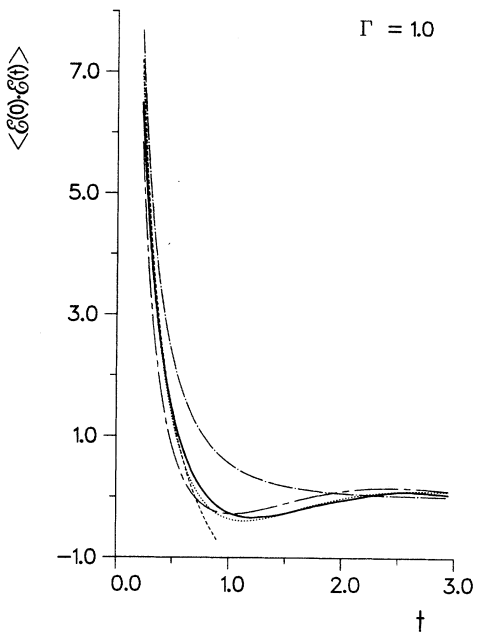

FIG. 4. The autocorrelation function $\langle \mathcal{E}(0)\cdot\mathcal{E}(t)\rangle$ of the electric field at $\Gamma=1$. $\langle \mathcal{E}(0)\cdot\mathcal{E}(t)\rangle$ and t are in units of e^2/a^4 and τ_0, respectively. Solid line, MD; dotted line, APEX; dashed line, small-time expansion (2.18); short-dashed–long-dashed line, mean-force; dash-dotted line, Brissaud-Frisch.

[through (3.37)] an APEX covariance $\Gamma^{AP}(t)$, whose small-term expansion reproduces the exact one (2.18) up to the constant term included. The free parameter η_A in (3.38) is now determined through a compromise between the location of the first zero and the amplitude of the negative first oscillation in $\Gamma^{AP}(t)$ compared to their MD counterparts.[28] The two other APEX parameters κ_A/κ_D and $(d\omega_A/dk)(\kappa_D/\omega_P)$ are computed from the fits[29] of $u_{exc}(\Gamma)$ and χ_T^0/χ_T as (4.4) and

$$\frac{\kappa_D}{\omega_P}\frac{d\omega_A}{dk}=\begin{cases}0.420\\ -0.184\\ -0.478\ ,\end{cases}\qquad \Gamma=\begin{cases}1\\ 5\\ 10\ ,\end{cases} \tag{4.8}$$

respectively. We then find

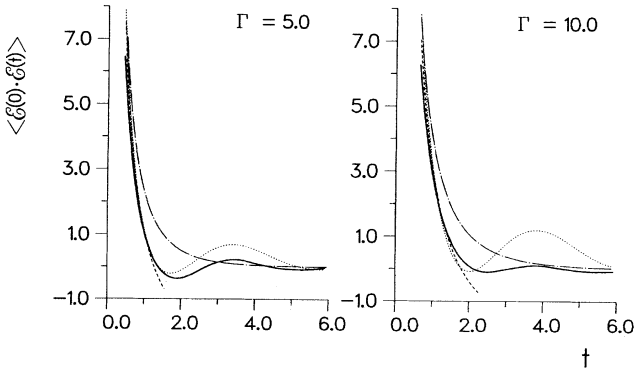

FIG. 5. The same as Fig. 4 at $\Gamma=5$ and 10, without the mean-force curve.

$$\eta_A = \begin{cases} 1.9 \\ 0.4 \\ 0.24 \end{cases}, \quad \Gamma = \begin{cases} 1 \\ 5 \\ 10 \end{cases}. \tag{4.9}$$

The curves representing $\Gamma^{\mathrm{AP}}(t)$ are shown in Figs. 4 and 5. At $\Gamma=1$, the APEX form is quite good and is better than the mean-force one. At $\Gamma=5$, $\Gamma^{\mathrm{AP}}(t)$ almost fits the MD results up to the first zero of $\Gamma(t)$. However, the positive second oscillation of $\Gamma^{\mathrm{AP}}(t)$ (which has the right location) is too large by a factor 3. At $\Gamma=10$, the MD $\Gamma(t)$ tends to be monotonic in the sense that its oscillations have very small amplitudes. The APEX representation fails in describing this peculiar behavior, since the oscillations in $\Gamma^{\mathrm{AP}}(t)$ remain rather large (except the negative first one, of course).

As in APEX, $\Gamma(t)$ is used as an ingredient in the Brissaud and Frisch model for $P(\mathbf{E}t|\mathbf{E}_0 0)$ which is described in Appendix C. The Brissaud and Frisch covariance reads

$$\Gamma^{\mathrm{BF}}(t)=\int_0^\infty dE\, E^2 P^{\mathrm{BF}}(E)\exp[-\nu(E)t]\,, \tag{4.10}$$

where the field-dependent jumping time density $\nu(E)$ has to be determined from the exact data relative to $\Gamma(t)$. Since $\Gamma^{\mathrm{BF}}(t)$ obviously is always positive, the oscillations of $\Gamma(t)$ cannot be reproduced by any choice of $\nu(E)$. Therefore, and for the sake of simplicity in the calculations, we just require that $\Gamma^{\mathrm{BF}}(t)$ reduces to the expression

$$\Gamma^{\mathrm{BF}}(t)=\frac{4(2\pi\beta m)^{1/2}e^2\rho}{t}\exp\left[\left[\frac{2\pi}{3}\right]^{1/2}\frac{u_{\mathrm{exc}}(\Gamma)}{\Gamma^{3/2}}\omega_p t\right], \tag{4.11}$$

which reproduces the short-time expansion (2.18) up to the constant term included. The corresponding $\nu(E)$ is given by (see Appendix C)

$$\nu(E)=\omega_P\left[-\left[\frac{2\pi}{3}\right]^{1/2}\frac{u_{\mathrm{exc}}(\Gamma)}{\Gamma^{3/2}} + \frac{1}{4(2\pi)^{1/2}e^2\rho\kappa_D}\int_0^E dE' E'^2 P^{\mathrm{BF}}(E')\right]. \tag{4.12}$$

The functions $\Gamma^{\mathrm{BF}}(t)$ are represented in Figs. 4 and 5. At small times, the agreement with the MD results is of course satisfactory. At intermediate times ($\tau_0 \le t \le 5\tau_0$), the comparisons with the MD data are very poor because of the absence of oscillations in $\Gamma^{\mathrm{BF}}(t)$.

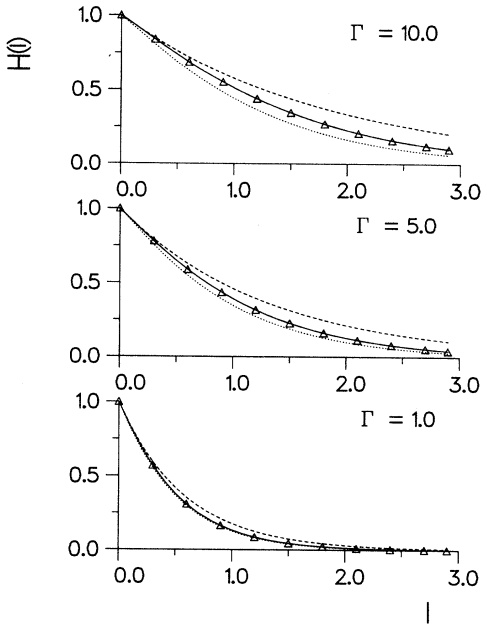

FIG. 6. The Fourier transform $H(l)$ of the probability distribution of the time derivative of the electric field at $\Gamma=1$, 5, and 10. l is in units of $(ma^7/e^4)^{1/2}$. Solid line and triangles, MD; dotted line, exponentiated response; dashed line, free particles.

2. *The probability distribution $G(f)$ of the time derivative of the field*

The Fourier transform $H(l)$ of $G(f)$ evaluated by MD is presented in Fig. 6 for the three values of Γ. The statistical error on this function is of the order of 2% and the domain of l where the values of $H(l)$ are significant corresponds to $l<5\tau_0 a^2/e$. The function $H(l)$ is monotonically decaying, with a kink at $l=0$. The decay is faster when Γ is lowered. This implies that $G(f)$ then shifts to high values of f and broadens.

The effective-field descriptions of $A_t(\mathbf{K},\mathbf{Q})$ provide approximate representations of $H(l)$ through the identity (2.25). We find

$$H^{\mathrm{MF,AP}}(l)=\lim_{t\to 0}A_t^{\mathrm{MF,AP}}\left[\frac{l}{t},-\frac{l}{t}\right]=\exp\left[4\pi\rho e\int_0^\infty dr\frac{1}{e_0^{\mathrm{MF,AP}}(r)}\left[\frac{\sin\{l[\partial e_t^{\mathrm{MF,AP}}(r)/\partial t]|_{t=0}\}}{l[\partial e_t^{\mathrm{MF,AP}}(r)/\partial t]|_{t=0}}-1\right]\right], \tag{4.13}$$

where the last line of (4.13) follows from the replacement of $A_t^{\mathrm{MF,AP}}(l/t,-l/t)$ by (3.12) with $\mathbf{e}_t^*(\mathbf{r})=\mathbf{e}_t^{\mathrm{MF,AP}}(\mathbf{r})$ and $\mathbf{K}=-\mathbf{Q}=l/t$. In the mean-force scheme, $\partial e_t^{\mathrm{MF}}(r)/\partial t|_{t=0}$ identically vanishes and consequently $H^{\mathrm{MF}}(l)$ reduces to 1. In the APEX scheme, $\partial e_t^{\mathrm{AP}}(r)/\partial t$ diverges when t goes to zero at any $r\neq 0$. We then find $H^{\mathrm{AP}}(0)=1$ and $H^{\mathrm{AP}}(l)=0$ for $l\neq 0$. Both mean-force and APEX forms of $H(l)$ turn out to be quite bad.

In fact, specific approximations for $H(l)$ can be derived from Eq. (2.26), independently of the general effective-field approaches mentioned above. The first one is equivalent to the Holtsmark treatment of $T(K)$ and

amounts to neglect of the interactions between the particles. The corresponding free-particle expression of $H(l)$ is

$$H^{\mathrm{fr}}(l)=\exp\left[-\left[1+\frac{\arg\sinh\sqrt{3}}{2\sqrt{3}}\right]\left[\frac{\pi e^2}{2\beta m a^6}\right]^{1/2} l\right]. \tag{4.14}$$

As shown in Appendix D, a second one can be obtained by starting from the integral representation of $H(l)$ over the coupling parameter λ varying from 0 to l^2. In this representation, the particles of the system are coupled to an external potential with magnitude proportional to λ, which can be interpreted as the potential created by a fictitious scatterer fixed at the origin. Making a simple ansatz (inspired by linear-response theory) for the corresponding pair correlation $g_\lambda(r)$ between the scatterer and one particle, we find (see Appendix D) the exponentiated-response (ER) expression

$$H^{\mathrm{ER}}(l)=\exp\left[-\frac{3}{2}\left[1+\frac{\arg\sinh\sqrt{3}}{2\sqrt{3}}\right]\frac{e^2}{\beta m a^3}\times\int_0^{l^2}d\lambda\int_0^{\infty}dr\frac{1}{r^4}g_\lambda^{\mathrm{ER}}(r)\right], \tag{4.15}$$

where $g_\lambda^{\mathrm{ER}}(r)$ is given by (D9). Both approximate forms (4.14) and (4.15) are represented in Fig. 6. The free (fr) approximation is qualitatively correct but overestimates $H(l)$. The corresponding distribution $4\pi f^2 G^{\mathrm{fr}}(f)$ of the modulus of $\mathbf{f}$ has a maximum whose location and width are too small. The exponentiated-response form improves over the free one. At $\Gamma=1$, the accuracy of the former is excellent. At $\Gamma=5,10$, this accuracy becomes less spectacular, but the overall quantitative agreement with the MD data remains quite reasonable.

D. The full time-dependent joint probability

The direct evaluation of $P(\mathbf{E}t|\mathbf{E}_0 0)$ by MD would be rather involved; so for the purpose of the comparison between theory and simulation, we have calculated the equivalent quantity $A_t(\mathbf{K},\mathbf{Q})$. A part of the MD data are given in Tables I–III. The limit behavior (2.12) of $A_t(\mathbf{K},\mathbf{Q})$ when $t\to\infty$ is reached within statistical error for $t\geq\tau_0$ and $t\geq 2\tau_0, 3\tau_0$, respectively for $\Gamma=1$ and $\Gamma=5,10$; these results give a reliable estimate of the relaxation time of $A_t(\mathbf{K},\mathbf{Q})$ at these couplings. The relaxation of $A_t(\mathbf{K},\mathbf{Q})$ is generally monotonic when $\mathbf{K}$ and $\mathbf{Q}$ are such that $T(|\mathbf{K}+\mathbf{Q}|)$ is larger than $T(K)T(Q)$. When this last relation is not verified the relaxation can show strongly damped oscillations. The data in the tables show that the range of values of K and Q where $A_t(\mathbf{K},\mathbf{Q})$ differs significantly from the statistical noise is between 0 and $5a^2/e$.

The mean-force and APEX forms of $A_t(\mathbf{K},\mathbf{Q})$ can be rewritten from (3.12) with $\mathbf{e}_t^{\mathrm{MF,AP}}(\mathbf{r})$ in place of $\mathbf{e}_t^*(\mathbf{r})$ as

TABLE I. The Fourier transform $A_t(\mathbf{K},\mathbf{Q})$ of the joint probability density $P(\mathbf{E}t|\mathbf{E}_0 0)$ at $\Gamma=1$, for various values of K,Q (in units of a^2/e) and θ as a function of the time t (in units of τ_0). Each line corresponds to a given set (K,Q,θ) while each column corresponds to a given time. In each box: top-left corner, MD; top-right corner, APEX; bottom-left corner, mean-force; bottom-right corner, Brissaud-Frisch.

K	Q	θ	0		0.15		0.30		0.50		0.80		1.0		∞	
			0.786	0.780												
0.5	0.0	0	0.805	0.780												
			0.677	0.672	0.650	0.655	0.649	0.619	0.629	0.609	0.617	0.607	0.615	0.607	0.617	0.608
0.5	0.5	$\pi/2$	0.713	0.672	0.707	0.642	0.652	0.628	0.649	0.619	0.648	0.613	0.648	0.610	0.648	0.608
			0.491	0.484	0.483	0.465	0.467	0.437	0.443	0.419	0.424	0.417	0.421	0.417	0.421	0.416
0.5	1.0	$\pi/2$	0.546	0.484	0.543	0.457	0.484	0.443	0.477	0.432	0.476	0.425	0.476	0.421	0.476	0.416
			0.200	0.204	0.200	0.195	0.195	0.185	0.182	0.172	0.167	0.169	0.166	0.169	0.164	0.168
0.5	2.0	$\pi/2$	0.276	0.204	0.275	0.192	0.245	0.186	0.234	0.180	0.233	0.176	0.233	0.173	0.233	0.168
			0.536	0.534												
1.0	0.0	0	0.591	0.534												
			0.272	0.279	0.273	0.270	0.276	0.260	0.276	0.265	0.284	0.292	0.290	0.301	0.287	0.285
1.0	1.0	$\pi/3$	0.353	0.279	0.353	0.270	0.289	0.268	0.325	0.269	0.366	0.273	0.370	0.275	0.350	0.285
			0.373	0.374	0.364	0.351	0.345	0.316	0.318	0.290	0.292	0.286	0.289	0.286	0.287	0.285
1.0	1.0	$\pi/2$	0.445	0.374	0.443	0.344	0.369	0.327	0.350	0.313	0.349	0.300	0.349	0.296	0.350	0.285
			0.274	0.279	0.268	0.247	0.226	0.198	0.175	0.141	0.126	0.111	0.112	0.104	0.111	0.115
1.0	2.0	$2\pi/3$	0.353	0.279	0.353	0.241	0.300	0.215	0.205	0.189	0.158	0.163	0.152	0.151	0.170	0.115
			0.208	0.216												
2.0	0.0	0	0.289	0.216												
			0.084	0.094	0.077	0.082	0.070	0.067	0.061	0.051	0.047	0.047	0.042	0.047	0.043	0.047
2.0	2.0	$\pi/2$	0.152	0.094	0.152	0.082	0.127	0.075	0.087	0.068	0.085	0.060	0.084	0.057	0.083	0.047
			0.218	0.216	0.195	0.177	0.149	0.119	0.094	0.065	0.049	0.043	0.040	0.039	0.043	0.047
2.0	2.0	$2\pi/3$	0.289	0.216	0.289	0.181	0.245	0.156	0.125	0.129	0.073	0.100	0.067	0.089	0.083	0.047
			0.018	0.023	0.015	0.021	0.015	0.019	0.013	0.016	0.010	0.013	0.010	0.014	0.011	0.012
4.0	1.0	$\pi/2$	0.052	0.023	0.052	0.021	0.046	0.019	0.036	0.018	0.035	0.017	0.028	0.016	0.034	0.012

TABLE II. The same as Table I at $\Gamma=5$ without the mean-force results.

K	Q	θ	0		0.40		0.80		1.00		2.00		∞
			0.814	0.795									
0.5	0.0	0		0.795									
			0.724	0.697	0.709	0.671	0.684	0.642	0.675	0.637	0.659	0.633	0.662	0.632
0.5	0.5	$\pi/2$		0.697		0.661	0.68	0.684		0.643		0.634		0.632
			0.562	0.523	0.549	0.501	0.523	0.470	0.509	0.462	0.489	0.454	0.494	0.453
0.5	1.0	$\pi/2$		0.523		0.487		0.517		0.467		0.456		0.453
			0.290	0.248	0.287	0.234	0.271	0.226	0.262	0.219	0.244	0.209	0.244	0.207
0.5	2.0	$\pi/2$		0.248		0.234		0.250		0.219		0.211		0.207
			0.607	0.569										
1.0	0.0	0		0.569										
			0.369	0.325	0.366	0.313	0.366	0.296	0.367	0.294	0.380	0.309	0.368	0.324
1.0	1.0	$\pi/3$		0.325		0.312		0.310		0.311		0.315		0.324
			0.460	0.418	0.443	0.393	0.411	0.354	0.395	0.341	0.363	0.326	0.368	0.324
1.0	1.0	$\pi/2$		0.418		0.377		0.356		0.349		0.331		0.324
			0.370	0.325	0.336	0.293	0.264	0.245	0.229	0.219	0.164	0.164	0.182	0.148
1.0	2.0	$2\pi/3$		0.33		0.266		0.230		0.217		0.177		0.148
			0.300	0.261										
2.0	0.0	0		0.261										
			0.158	0.129	0.150	0.117	0.128	0.101	0.117	0.091	0.081	0.071	0.090	0.068
2.0	2.0	$\pi/2$		0.129		0.108		0.096		0.091		0.071		0.068
			0.306	0.261	0.252	0.222	0.165	0.165	0.131	0.135	0.074	0.080	0.090	0.068
2.0	2.0	$2\pi/3$		0.261		0.201		0.163		0.149		0.078		0.068
			0.050	0.040	0.049	0.037	0.045	0.033	0.041	0.032	0.031	0.030	0.033	0.025
4.0	1.0	$\pi/2$		0.040		0.035		0.031		0.031		0.028		0.025

TABLE III. The same as Table II at $\Gamma=10$.

K	Q	θ	0		0.40		0.80		1.00		2.00		∞
			0.822	0.799									
0.5	0.0	0		0.799									
			0.739	0.704	0.729	0.688	0.712	0.662	0.702	0.653	0.680	0.641	0.675	0.640
0.5	0.5	$\pi/2$		0.704		0.674		0.660		0.655		0.644		0.640
			0.585	0.533	0.578	0.519	0.516	0.500	0.551	0.488	0.518	0.467	0.517	0.463
0.5	1.0	$\pi/2$		0.533		0.503		0.488		0.483		0.470		0.463
			0.325	0.261	0.324	0.253	0.315	0.245	0.309	0.242	0.278	0.224	0.273	0.219
0.5	2.0	$\pi/2$		0.261		0.245		0.237		0.234		0.225		0.219
			0.629	0.579										
1.0	0.0	0		0.579										
			0.403	0.337	0.401	0.327	0.401	0.314	0.403	0.305	0.404	0.294	0.395	0.335
1.0	1.0	$\pi/3$		0.337		0.326		0.332		0.322		0.324		0.335
			0.489	0.430	0.479	0.414	0.456	0.393	0.443	0.377	0.394	0.343	0.395	0.335
1.0	1.0	$\pi/2$		0.430		0.397		0.376		0.369		0.348		0.335
			0.403	0.337	0.380	0.322	0.324	0.302	0.296	0.288	0.204	0.221	0.208	0.158
1.0	2.0	$2\pi/3$		0.337		0.289		0.257		0.244		0.202		0.158
			0.332	0.274										
2.0	0.0	0		0.274										
			0.191	0.139	0.180	0.132	0.159	0.124	0.153	0.120	0.109	0.088	0.111	0.075
2.0	2.0	$\pi/2$		0.139		0.121		0.109		0.105		0.080		0.075
			0.335	0.273	0.300	0.256	0.231	0.232	0.200	0.219	0.107	0.137	0.111	0.075
2.0	2.0	$2\pi/3$		0.273		0.224		0.190		0.176		0.129		0.075
			0.071	0.032	0.069	0.069	0.063	0.041	0.061	0.041	0.043	0.035	0.047	0.029
4.0	1.0	$\pi/2$		0.032		0.041		0.038		0.037		0.033		0.029

$$A_t^{\mathrm{MF,AP}}(\mathbf{K},\mathbf{Q})=\exp\left[2\pi\rho e\int_0^\infty dr\frac{1}{e_0^{\mathrm{MF,AP}}(r)}\left\{\frac{\sin[|\mathbf{K}e_t^{\mathrm{MF,AP}}(r)+\mathbf{Q}e_0^{\mathrm{MF,AP}}(r)|]}{|\mathbf{K}e_t^{\mathrm{MF,AP}}(r)+\mathbf{Q}e_0^{\mathrm{MF,AP}}(r)|}+\frac{\sin[|\mathbf{Q}e_t^{\mathrm{MF,AP}}(r)+\mathbf{K}e_0^{\mathrm{MF,AP}}(r)|]}{|\mathbf{Q}e_t^{\mathrm{MF,AP}}(r)+\mathbf{K}e_0^{\mathrm{MF,AP}}(r)|}+\frac{\sin[Ke_0^{\mathrm{MF,AP}}(r)]}{Ke_0^{\mathrm{MF,AP}}(r)}+\frac{\sin[Qe_0^{\mathrm{MF,AP}}(r)]}{Qe_0^{\mathrm{MF,AP}}(r)}-\frac{\sin[Ke_t^{\mathrm{MF,AP}}(r)]}{Ke_t^{\mathrm{MF,AP}}(r)}-\frac{\sin[Qe_t^{\mathrm{MF,AP}}(r)]}{Qe_t^{\mathrm{MF,AP}}(r)}-2\right\}\right], \tag{4.16}$$

where the effective fields are given by

$$e_t^{\mathrm{MF}}(r)=\frac{2e}{\pi r}\int_0^\infty dk\left[\frac{\sin(kr)}{kr}-\cos(kr)\right]\tilde{S}_{3P}(k,t)\ , \tag{4.17a}$$

$$e_t^{\mathrm{AP}}(r)=\frac{2e}{\pi r}\int_0^\infty dk\left[\frac{\sin(kr)}{kr}-\cos(kr)\right]\tilde{D}_A(k,t)\ . \tag{4.17b}$$

The expressions (4.17a) and (4.17b) are readily obtained by replacing the convolution integrals in the rhs of (3.18) and (3.31), by integrals over $\mathbf{k}$ of the product of the Fourier transforms of the bare Coulomb field $\mathbf{e}(\mathbf{r}')$ and of the space distributions $S(|\mathbf{r}'-\mathbf{r}|,t)$ and $D_A(|\mathbf{r}'-\mathbf{r}|,t)$. Moreover, $\tilde{S}_{3P}(k,t)$ and $\tilde{D}_A(k,t)$ are determined through the sets of equations (3.21)–(3.26) and (3.33), (3.38), respectively, while the APEX parameters are given in Eqs. (4.4), (4.8), and (4.9) for the three considered values of Γ. The Brissaud and Frisch form for $A_t(\mathbf{K},\mathbf{Q})$ is derived in Appendix C with the result

$$A_t^{\mathrm{BF}}(\mathbf{K},\mathbf{Q})=T^{\mathrm{BF}}(K)T^{\mathrm{BF}}(Q)+\int_0^\infty dE\,P^{\mathrm{BF}}(E)\exp[-\nu(E)t]\frac{\sin(|\mathbf{K}+\mathbf{Q}|E)}{|\mathbf{K}+\mathbf{Q}|E}-\int_0^\infty dE\int_0^\infty dE_0 P^{\mathrm{BF}}(E)P^{\mathrm{BF}}(E_0)\frac{\sin(KE_0)}{KE_0}\frac{\sin(QE)}{QE}\times\left[\frac{\nu(E_0)[\nu(E)-\langle\nu\rangle^{\mathrm{BF}}]}{\langle\nu\rangle^{\mathrm{BF}}[\nu(E)-\nu(E_0)]}\exp[-\nu(E)t]+\frac{\nu(E)}{\langle\nu\rangle^{\mathrm{BF}}}\frac{[\nu(E_0)-\langle\nu\rangle^{\mathrm{BF}}]}{[\nu(E_0)-\nu(E)]}\exp[-\nu(E_0)t]\right]. \tag{4.18}$$

The static distribution $P^{\mathrm{BF}}(E)$ of the modulus of the electric microfield plays the role of an ingredient in the Brissaud and Frisch theory. Here, we choose $P^{\mathrm{BF}}(E)$ equal to $P^{\mathrm{AP}}(E)$, which is the best approximate representation of the exact distribution (see Sec. IV B). The jumping density $\nu(E)$ is then given by (4.12) with $P^{\mathrm{BF}}(E)=P^{\mathrm{AP}}(E)$. The latter choice of $P^{\mathrm{BF}}(E)$ implies that $A_t^{\mathrm{BF}}(\mathbf{K},\mathbf{Q})$ and $A_t^{\mathrm{AP}}(\mathbf{K},\mathbf{Q})$ have the same static limits at $t=0$ and $t=\infty$.

Tables I–III summarize the comparison of theory and simulation for various values of K,Q and of the angle θ between $\mathbf{K}$ and $\mathbf{Q}$. At $\Gamma=1$, the agreement between simulations and theory is satisfactory. The mean-force approximation cannot be very accurate because its description of the static limits is only semiquantitative (see Sec. IV B); however, it reproduces the qualitative variations of $A_t(\mathbf{K},\mathbf{Q})$ with respect to t. The APEX and Brissaud-Frisch theories give more accurate results. For angles between $\pi/3$ and $2\pi/3$, the oscillatory behavior of $A_t(\mathbf{K},\mathbf{Q})$ observed in MD is not well described by the BF form which is almost monotonic. The APEX form has the right oscillations but their amplitude is overestimated. For angles close to 0 or π ($\mathbf{K}$ parallel or antiparallel to $\mathbf{Q}$), APEX is slightly more accurate than BF, and its overall agreement with the MD results is quite reasonable (see Fig. 7). At $\Gamma=5,10$ the above qualitative features remain almost unchanged, with the only difference that the MD $A_t(\mathbf{K},\mathbf{Q})$ exhibits less structure than at $\Gamma=1$. For these values of Γ, the predictions of APEX and BF are only semiquantitative (see Tables II and III). Finally,

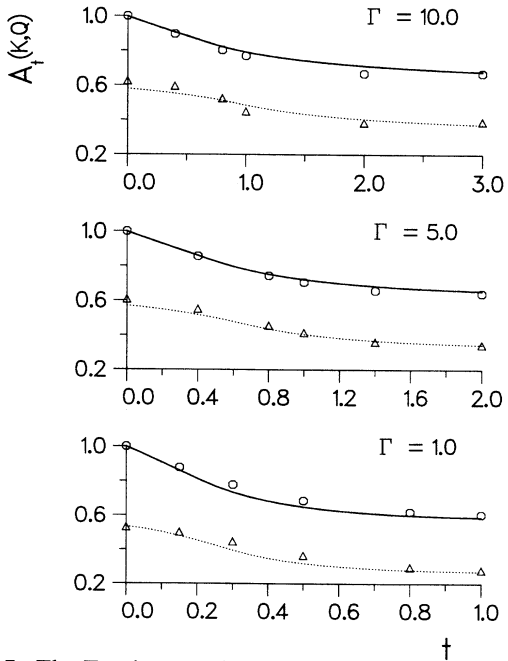

FIG. 7. The Fourier transform $A_t(\mathbf{K},\mathbf{Q})$ of the joint probability density $P(\mathbf{E}t|\mathbf{E}_0 0)$ at $\Gamma=1$, 5, and 10, for two sets of values of (K,Q,θ) with $\theta=\arccos(\hat{\mathbf{K}}\cdot\hat{\mathbf{Q}})$. The time t is in units of τ_0. Open circles, MD; solid line, APEX (results for $K=Q=a^2/e$ and $\theta=\pi$). Open triangles, MD; dotted line, APEX (results for $K=Q=0.5a^2/e$ and $\theta=2\pi/3$).

APEX appears to be the most accurate theory. Its main shortcomings are, first, to overestimate both the variations of $A_t(\mathbf{K},\mathbf{Q})$ at small times ($t \leq 0.5\tau_0$) and the amplitude of its oscillations at intermediate times ($0.5\tau_0 \leq t \leq 1.5\tau_0$), second, to miss small large-time ($1.5\tau_0 \leq t$) oscillations when Γ increases.

V. CONCLUSION

The effective-field approach provides simple and reliable expressions for the Fourier transform $A_t(\mathbf{K},\mathbf{Q})$ of the joint probability density $P(\mathbf{E}t|\mathbf{E}_0 0)$. The mean-force version of this approach has a range of validity which is restricted to the weak-coupling regime (Γ small), because its description of the static limits at zero and infinite time becomes rather poor when Γ increases. The APEX effective-field theory overcomes this defect and remains reasonably accurate in the intermediate coupling regime ($1 \leq \Gamma \leq 10$). In particular, APEX reproduces the oscillatory behavior of $A_t(\mathbf{K},\mathbf{Q})$ which is linked to the plasmon oscillations. Moreover, this theory relies on a very few ingredients which, in a simplified version, can be ultimately expressed in terms of the excess internal energy $u_{\text{exc}}(\Gamma)$ only (see Refs. 28 and 29).

Despite its rather crude representation of the dynamics of the microfield, the Brissaud and Frisch model gives reasonable results for $A_t(\mathbf{K},\mathbf{Q})$, if one uses the APEX form of the static distribution $T(K)$ [these results should be improved by including in $T(K)$ the first corrections to APEX calculated in Ref. 16]. In fact, similarly to what happens in the case of the time-displaced particle correlations (see Ref. 20, for instance), a good description of the static limits guarantees a minimal accuracy at intermediate times (this also explains in part the success of the dynamical APEX theory). The Brissaud and Frisch model is not as accurate as the APEX effective-field approach, for the main reason that it misses the oscillatory behaviors of $A_t(\mathbf{K},\mathbf{Q})$ and of the covariance $\Gamma(t)$ (however, the quantitative differences between both approximations are not very spectacular because the amplitudes of the corresponding oscillations turn out to be rather small). Moreover, the former theory predicts that the zero-time delta peak $\delta(\mathbf{E}-\mathbf{E}_0)$ in $P(\mathbf{E}t|\mathbf{E}_0 0)$ survives for all times with an exponentially decaying amplitude (see Appendix C), whereas APEX correctly describes (from a qualitative point of view) the shifting and broadening of this peak at $t \neq 0$.

Although the global predictions relative to $P(\mathbf{E}t|\mathbf{E}_0 0)$ of the APEX theory are satisfactory, one has to be careful when calculating reduced dynamical quantities within this approximation. This is well illustrated by the case of the distribution $G(f)$ of the time derivative of the microfield, which is poorly represented by APEX [similar results should also be observed for the conditional moments of Chandrasekhar and von Neumann[13] which can be deduced from $\lim_{t\to 0} A_t(\mathbf{K}+1/t,-1/t)$]. In fact, specific representations of the above quantities should be useful for improving the present choice of the APEX effective-field $\mathbf{e}_t^{\text{AP}}(\mathbf{r})$. For instance, the exponentiated-response form of $G(f)$ and a hydrodynamic expression [via $S(k,t)$] of the autocorrelation function $\Gamma(t)$ provide constraints on, respectively, the small- and large-time behaviors of $\mathbf{e}_t^{\text{AP}}(\mathbf{r})$ [the present APEX description of $\Gamma(t)$ at large times becomes poor when Γ increases].

Compared to other theories the effective-field approach has the following main advantages. First, this method directly provides explicit expressions for the quantities of interest without having to solve complicated evolution equations as would be the case in a standard kinetic theory. Second, it allows one to incorporate, in a phenomenological way, the essential features of the particle dynamics like, for instance, the screening effects[30] or the plasmon oscillations and the qualitative shapes of the related dispersion curves. This cannot be done in approaches of the Brissaud-Frisch type which "forget" the origin of the microfield. Finally, the flexibility in the choice of the effective field should be useful in the application of the theory to other situations than the one studied in this paper, e.g., multicomponent systems or radiating ions [in the latter case $\mathcal{E}(t)$ would be the electric field "seen" by a moving charge of the system].

Recently, Dufty and Zogaib[31] have introduced an independent-particle model for describing $A_t(\mathbf{K},\mathbf{Q})$ which is similar to our approach. In their model, $A_t(\mathbf{K},\mathbf{Q})$ is expressed in terms of a static effective field $\mathbf{e}_0^*(\mathbf{r})$ via a suitable renormalization of a generalized Baranger-Mozer cluster expansion of $\ln[A_t(\mathbf{K},\mathbf{Q})]$ (this procedure extends to the dynamical case the method used for dealing with the static distribution[16]). In this model, the dynamics of the charges is incorporated in the correlations between particle densities at different times and points $\mathbf{r}$ and $\mathbf{r}'$ which are multiplied by weight factors $\{\exp[i\mathbf{K}\cdot\mathbf{e}_0^*(\mathbf{r})]-1\}$ and $\{\exp[i\mathbf{Q}\cdot\mathbf{e}_0^*(\mathbf{r}')]-1\}$ in integrals over $\mathbf{r}$ and $\mathbf{r}'$. In our approach, such dynamics are incorporated in the effective field itself which is time dependent.

As far as line-shape calculations are concerned, it has been shown in the literature[6,7,32] that the Brissaud and Frisch model may give satisfactory results. Our study is compatible with this observation, since the corresponding description of the dynamics of the microfield turns out to be semiquantitative. It is then tempting to think that the effective-field approach should be helpful for improving the Brissaud-Frisch calculations of spectral lines, especially when the latter show strong disagreements with experimental data[8] (of course these disagreements arise from various uncontrolled approximations and cannot be entirely removed through a better representation of the microfield dynamics). However, it still remains to derive tractable expressions of the frequency profiles in the framework of effective-field models. The simple expressions obtained in the BF theory are indeed very specific to the Kangaroo process.

ACKNOWLEDGMENTS

This work was supported in part by the U.S. Air Force Office of Scientific Research Grant No. 0010D. One of us (A.A.) is indebted to J.P. Hansen for his hospitality at the Ecole Normale Supérieure de Lyon. The Laboratoire de Physique Théorique et Hautes Energies is a "Laboratoire associé au Centre National de la Recherche Scientifique."

APPENDIX A

In this appendix, we study the small-time expansion of $\Gamma(t)$ and compute its first terms. For this, we start from the expression (2.16) of $\Gamma(t)$ where we split $\tilde{S}(k,t)$ in a "self" part $\tilde{S}_s(k,t)$ and a "distinct" part $\tilde{S}_d(k,t)$ given by

$$\rho\tilde{S}_s(k,t)=\int d\mathbf{r}\exp(i\mathbf{k}\cdot\mathbf{r})\left\langle\sum_{i=1}^{N}\delta(\mathbf{r}_i(t)-\mathbf{r})\delta(\mathbf{r}_i(0)-\mathbf{0})\right\rangle , \tag{A1}$$

$$\rho\tilde{S}_d(k,t)=\int d\mathbf{r}\exp(i\mathbf{k}\cdot\mathbf{r})\left[\left\langle\sum_{\substack{i,j=1\\ i\neq j}}^{N}\delta(\mathbf{r}_j(t)-\mathbf{r})\delta(\mathbf{r}_i(0)-\mathbf{0})\right\rangle-\rho^2\right] . \tag{A2}$$

Let $\Gamma_s(t)$ and $\Gamma_d(t)$ be the contributions of, respectively, the self (A1) and distinct (A2) parts of $\tilde{S}(k,t)$ to $\Gamma(t)$. The small-time expansion of $\Gamma_d(t)$ is easily inferred from the one of $\tilde{S}_d(k,t)$.

$$\tilde{S}_d(k,t)=\sum_{n=0}^{\infty}t^{2n}\tilde{S}_d^{(2n)}(k) , \tag{A3}$$

because all the functions $\tilde{S}_d^{(2n)}(k)$ are integrable with respect to k. Inserting (A3) in (2.16) and inverting the sum over n and the integral over k, we then obtain the required expansion of $\Gamma_d(t)$,

$$\Gamma_d(t)=8e^2\rho\sum_{n=0}^{\infty}t^{2n}\int_0^{\infty}dk\,\tilde{S}_d^{(2n)}(k) , \tag{A4}$$

which contains only even powers of t. The first two terms in the rhs of (A4) are immediately computed by using the fact that $\tilde{S}_d^{(0)}(k)/\rho$ is nothing but the Fourier transform of the Ursell function $h(r)$ while $\tilde{S}_d^{(2)}(k)$ vanishes [the t^2 term in the expansion of the full $\tilde{S}(k,t)$ entirely arises from free motion and does not depend on the interactions]. We find

$$\Gamma_d(t)=8\pi\rho k_B T u_{\mathrm{exc}}(\Gamma)+O(t^4) , \tag{A5}$$

where $u_{\mathrm{exc}}(\Gamma)$ is the excess internal energy of the OCP in units of $k_B T$,

$$u_{\mathrm{exc}}(\Gamma)=\frac{\beta\rho}{2}\int d\mathbf{r}\frac{e^2}{r}h(r)$$
$$=\frac{\beta e^2}{\pi}\int_0^{\infty}dk\,\tilde{S}_d^{(0)}(k) \tag{A6}$$

[the last line of (A6) follows from Parseval's theorem].

The expansion of $\Gamma_s(t)$ cannot be obtained by a simple term-by-term integration over k of the expansion of $\tilde{S}_s(k,t)$ in powers of t because the involved functions of k do not decay when $k\to\infty$. For instance, one has $\tilde{S}_s^{(0)}(k)=1$ which is obviously nonintegrable. This difficulty reflects the singular behavior of $\Gamma_s(t)$ when $t\to 0$ which is linked to the divergence of $\Gamma(0)=\langle[\mathscr{E}(0)]^2\rangle$ (the latter arises from "self" contributions of particles close to the considered neutral point). In order to determine this behavior, it is in fact more appropriate to expand $\tilde{S}_s(k,t)$ around its "free-gas" expression $\exp(-k^2t^2/2m\beta)$. First, the definition (A1) can be rewritten as

$$\tilde{S}_s(k,t)=\int d\mathbf{v}_1\varphi(v_1)\langle\exp[i\mathbf{k}\cdot\mathbf{r}_1(t)]\rangle_0^1 , \tag{A7}$$

where $\varphi(v)=(\beta m/2\pi)^{3/2}\exp(-\beta mv^2/2)$ is the normalized Maxwellian distribution of the velocities, $\mathbf{r}_1(t)$ is the position of particle 1 at time t with the initial conditions $\mathbf{r}_1(0)=\mathbf{0}$ and $\mathbf{v}_1(0)=\mathbf{v}_1$, and the measure which defines the average $\langle\ \rangle_0^1$ is

$$\frac{d\mathbf{r}_2\cdots d\mathbf{r}_N d\mathbf{v}_2\cdots d\mathbf{v}_N\varphi(\mathbf{v}_2)\cdots\varphi(\mathbf{v}_N)\exp[-\beta V(\mathbf{0},\mathbf{r}_2,\ldots,\mathbf{r}_N)]}{\int d\mathbf{r}_2\cdots d\mathbf{r}_N\exp[-\beta V(\mathbf{0},\mathbf{r}_2,\ldots,\mathbf{r}_N)]} . \tag{A8}$$

Let $\mathbf{s}_1(t)$ be the deviation from free motion at time t defined through

$$\mathbf{r}_1(t)=\mathbf{v}_1 t+\mathbf{s}_1(t) . \tag{A9}$$

Inserting (A9) in (A7) and taking into account that the measure (A8) does not depend on $\mathbf{v}_1$, we obtain

$$\tilde{S}_s(k,t)=\int d\mathbf{v}_1\varphi(v_1)\exp(i\mathbf{k}\cdot\mathbf{v}_1 t)\langle\exp[i\mathbf{k}\cdot\mathbf{s}_1(t)]\rangle_0^1$$

$$=\int d\mathbf{v}_1\varphi(v_1)\exp(i\mathbf{k}\cdot\mathbf{v}_1 t)\left[1+\sum_{n=1}^{\infty}\frac{1}{n!}\langle[i\mathbf{k}\cdot\mathbf{s}_1(t)]^n\rangle_0^1\right] . \tag{A10}$$

The Taylor expansion of $\mathbf{s}_1(t)$ around $t=0$ reads

$$\mathbf{s}_1(t)=\sum_{p=2}^{\infty}\frac{t^p}{p!}\frac{d^p\mathbf{s}_1}{dt^p}(0) \tag{A11}$$

[$\mathbf{s}_1(0)$ and $d\mathbf{s}_1/dt(0)$ vanish because of the definition (A9) of $\mathbf{s}_1(t)$]. The time derivatives $d^p\mathbf{s}_1/dt^p(0)$ can be calculated recursively from Newton's equations of motion,

$$m\frac{d^2}{dt^2}\mathbf{s}_1(t)=-\nabla_1 V(\mathbf{r}_1(t),\ldots,\mathbf{r}_N(t)) , \tag{A12}$$

as polynomials in the initial velocities $\mathbf{v}_1,\mathbf{v}_2,\ldots,\mathbf{v}_N$ with coefficients proportional to gradients of the total interaction potential V evaluated for the initial spatial configuration $(\mathbf{0},\mathbf{r}_2,\ldots,\mathbf{r}_N)$. These polynomials are odd with respect to the change of sign of all the velocities if p is odd, and they are even otherwise. Taking also into account the parity of $\varphi(v)$ with respect to the change of $\mathbf{v}$ in $-\mathbf{v}$, we then see that the short-time expansion of $\langle[i\mathbf{k}\cdot\mathbf{s}_1(t)]^n\rangle_0^1$ starts at the order t^{2n} at least, and the coefficient of the corresponding term of order t^q is a polynomial in $\mathbf{v}_1$ with the parity of q. Since, for obvious symmetry reasons, $\langle[i\mathbf{k}\cdot\mathbf{s}_1(t)]^n\rangle_0^1$ is an even (odd) function of $\mathbf{v}_1$ if n is even (odd), the above coefficient necessarily vanishes if q does not have the same parity as n. Therefore we get

$$\langle[i\mathbf{k}\cdot\mathbf{s}_1(t)]^n\rangle_0^1=\begin{cases}k^n t^{2n}\displaystyle\sum_{p=0}^{\infty}\mathcal{P}^p_{n,\hat{\mathbf{k}}}(\mathbf{v}_1)t^{2p}, & n \text{ even}\\ k^n t^{2n+1}\displaystyle\sum_{p=0}^{\infty}\mathcal{P}^p_{n,\hat{\mathbf{k}}}(\mathbf{v}_1)t^{2p}, & n \text{ odd}\end{cases} \tag{A13}$$

where $\mathcal{P}^p_{n,\hat{\mathbf{k}}}(\mathbf{v}_1)$ is a polynomial in $\mathbf{v}_1$ with coefficients which depend on n and $\hat{\mathbf{k}}$; is n is even (odd), $\mathcal{P}^p_{n,\hat{\mathbf{k}}}(\mathbf{v}_1)$ is even (odd) in $\mathbf{v}_1$ and of order $2p$ $(2p+1)$. Using (A13) in (A10) and inverting the discrete sums and the integration over $\mathbf{v}_1$, we find the required expansion of $\tilde{S}_s(k,t)$ as

$$\tilde{S}_s(k,t)=\exp(-k^2t^2/2m\beta)\left[1+\sum_{n=1}^{\infty}\frac{k^{2n}t^{4n}}{(2n)!}\sum_{p=0}^{\infty}Q^p_{2n}(kt)t^{2p}+\sum_{n=0}^{\infty}\frac{k^{2n+1}t^{4n+3}}{(2n+1)!}\sum_{p=0}^{\infty}Q^p_{2n+1}(kt)t^{2p}\right] , \tag{A14}$$

where $Q^p_{2n}(kt)$ $[Q^p_{2n+1}(kt)]$ is an even (odd) polynomial in kt of order $2p$ $(2p+1)$ defined through

$$\left[\frac{\beta m}{2\pi}\right]^{3/2}\int d\mathbf{v}_1\exp(-\beta m\mathbf{v}_1^2/2)\mathcal{P}^p_{n,\hat{\mathbf{k}}}(\mathbf{v}_1)\exp(i\mathbf{k}t\cdot\mathbf{v}_1)=\exp(-k^2t^2/2m\beta)Q^p_n(kt) . \tag{A15}$$

[The Fourier transform of a Gaussian multiplied by a polynomial has the same structural form and $Q^p_n(kt)$ does not depend on $\hat{\mathbf{k}}$ because of the rotation invariance of the system.] The replacement of $\tilde{S}_s(k,t)$ by (A14) in (2.16) together with a term-by-term integration over k and the variable change $u=kt/(2m\beta)^{1/2}$ finally give

$$\Gamma_s(t)=\frac{4e^2\rho(2\pi m\beta)^{1/2}}{t}\left[1+\frac{2}{\pi^{1/2}}\sum_{n=1}^{\infty}\frac{(2m\beta)^n}{(2n)!}t^{2n}\sum_{p=0}^{\infty}t^{2p}\int_0^{\infty}du\,\exp(-u^2)u^{2n}Q^p_{2n}[(2m\beta)^{1/2}u]\right.$$
$$\left.+\frac{2}{\pi^{1/2}}\sum_{n=0}^{\infty}\frac{(2m\beta)^{n+1/2}}{(2n+1)!}t^{2n+2}\sum_{p=0}^{\infty}t^{2p}\int_0^{\infty}du\,\exp(-u^2)u^{2n+1}Q^p_{2n+1}[(2m\beta)^{1/2}u]\right] . \tag{A16}$$

The Laurent expansion (A16) of $\Gamma_s(t)$ contains only odd powers of t, and its singular $1/t$ term is entirely determined by the free motion. At a given order in t, one has to collect a finite number of contributions in the discrete sums over n and p. For instance, the linear term arises from the two contributions $(2n=2,\ p=0)$ and $(2n+1=1,\ p=0)$. Using the Taylor expansion (A11) of $\mathbf{s}_1(t)$, we find after a little algebra

$$\mathcal{P}^0_{1,\hat{\mathbf{k}}}(\mathbf{v}_1)=\frac{-i}{6m}\left\langle\sum_{j=1}^{N}(\mathbf{v}_j\cdot\nabla_j)(\hat{\mathbf{k}}\cdot\nabla_1)V(\mathbf{0},\mathbf{r}_2,\ldots,\mathbf{r}_N)\right\rangle_0^1$$
$$=-\frac{i}{18}\omega_p^2\hat{\mathbf{k}}\cdot\mathbf{v}_1 \tag{A17}$$

and

$$\mathcal{P}^0_{2,\hat{\mathbf{k}}}(\mathbf{v}_1)=\frac{-1}{4m^2}\langle[\hat{\mathbf{k}}\cdot\nabla_1 V(\mathbf{0},\mathbf{r}_2,\ldots,\mathbf{r}_N)]^2\rangle_0^1$$
$$=-\frac{1}{12m\beta}\omega_p^2 . \tag{A18}$$

Using (A17) and (A18) in (A15) we find $Q^0_1[(2m\beta)^{1/2}u]=\omega_p^2u/[9(2m\beta)^{1/2}]$ and $Q^0_2[(2m\beta)^{1/2}u]=-\omega_p^2/12m\beta$, from which we easily compute the related Gaussian integrals over u involved in (A16). The resulting expression for $\Gamma_s(t)$ is

$$\Gamma_s(t)=\frac{4e^2\rho(2\pi m\beta)^{1/2}}{t}\left[1+\frac{\omega_p^2t^2}{72}+O(t^4)\right] . \tag{A19}$$

The expression (2.18) for the full $\Gamma(t)$ is obtained by adding (A19) to (A5).

APPENDIX B

The three-pole expression of $\tilde{S}(k,\omega)$ is

$$\tilde{S}_{3P}(k,\omega)=\frac{\tau_{3P}(k)\omega_0^2(k)[\omega_{1l}^2(k)-\omega_{2l}^2(k)]}{\pi\{\omega^2\tau_{3P}^2(k)[\omega^2-\omega_{1l}^2(k)]^2+[\omega^2-\omega_{0l}^2(k)]^2\}} , \tag{B1}$$

where the frequencies $\omega_0(k), \omega_{0l}(k), \omega_{1l}(k)$ and the relaxation time $\tau_{3P}(k)$ are given in the text. The rational fraction in ω (B1) has three pairs of complex-conjugate poles which are the roots of

$$\omega^3 - \frac{i\omega^2}{\tau_{3P}(k)} - \omega\omega_{1l}^2(k) + i\frac{\omega_{0l}^2(k)}{\tau_{3P}(k)} = 0 , \tag{B2}$$

$$\omega^3 + \frac{i\omega^2}{\tau_{3P}(k)} - \omega\omega_{1l}^2(k) - i\frac{\omega_{0l}^2(k)}{\tau_{3P}(k)} = 0 . \tag{B3}$$

The three roots of (B2) take the form

$$\begin{aligned} \omega_1 &= \alpha + i\delta , \\ \omega_2 &= -\alpha + i\delta , \\ \omega_3 &= i\gamma , \end{aligned} \tag{B4}$$

where α, β, γ are real positive numbers, while their complex conjugates $\bar{\omega}_1 = -\omega_2$, $\bar{\omega}_2 = -\omega_1$, $\bar{\omega}_3 = -\omega_3$ are the three roots of (B3). The expression (3.23) of γ directly follows from the usual Cartan method for solving third-degree equations. The expression (3.25) for δ and (3.26) for α are then readily obtained by writing

$$\begin{aligned} \omega_1 + \omega_2 + \omega_3 &= \frac{i}{\tau_{3P}(k)} , \\ \omega_1\omega_2 + \omega_1\omega_3 + \omega_2\omega_3 &= \omega_{1l}^2(k) . \end{aligned} \tag{B5}$$

The three-pole expression of $\tilde{S}(k,t)$ is given by the Fourier transform with respect to ω of (B1), i.e., (for $t > 0$)

$$\begin{aligned} \tilde{S}_{3P}(k,\omega) &= \int_{-\infty}^{\infty} d\omega \exp(i\omega t) \frac{\omega_0^2(k)[\omega_{1l}^2(k) - \omega_{0l}^2(k)]}{\pi\tau_{3P}(k)(\omega-\omega_1)(\omega-\bar{\omega}_1)(\omega-\omega_2)(\omega-\bar{\omega}_2)(\omega-\omega_3)(\omega-\bar{\omega}_3)} \\ &= \frac{2i\omega_0^2(k)[\omega_{1l}^2(k) - \omega_{0l}^2(k)]}{\tau_{3P}(k)} \sum_{j=1}^{3} \frac{\exp(i\omega_j t)}{(\omega_j - \bar{\omega}_j) \prod_{l(\neq j)} (\omega_j - \omega_l)(\omega_j - \bar{\omega}_l)} , \end{aligned} \tag{B6}$$

where we have used Cauchy's theorem together with Jordan's lemma. The substitution of the roots $\omega_1, \omega_2, \omega_3$ by their forms (B4) in (B6) finally leads to the expression (3.21) for $\tilde{S}_{3P}(k,t)$.

APPENDIX C

In the Brissaud-Frisch model, the microfield $\mathcal{E}(t)$ is assumed to evolve according to a stepwise constant stochastic process: $\mathcal{E}(t)$ jumps from $\mathbf{E}_i$ to $\mathbf{E}_{i+1}$ at the jumping time t_{i+1}, and remains constant between two successive jumping times. The jumping times t_i are uniformly and independently distributed with density $\nu(\mathbf{E}_{i-1})$, while the constants $\mathbf{E}_i$ are random vectors chosen independently with the same probability distribution $W^{\mathrm{BF}}(E)$. This process is known as the Kangaroo process [the simplified version in which $\nu(E)$ reduces to a constant ν is called the Poisson-step process]. The corresponding Fokker-Planck equation which governs the evolution of $P^{\mathrm{BF}}(\mathbf{E}t|\mathbf{E}_0 0)$ reads

$$\begin{aligned} \frac{\partial P^{\mathrm{BF}}(\mathbf{E}t|\mathbf{E}_0 0)}{\partial t} &= -\nu(E) P^{\mathrm{BF}}(\mathbf{E}t|\mathbf{E}_0 0) \\ &\quad + Q(E) \int d\mathbf{E}' \nu(\mathbf{E}') P^{\mathrm{BF}}(\mathbf{E}'t|\mathbf{E}_0 0) , \end{aligned} \tag{C1}$$

with

$$Q(E) = \frac{\nu(E) W^{\mathrm{BF}}(E)}{\int d\mathbf{E}' \nu(E') W^{\mathrm{BF}}(E')} , \tag{C2}$$

and the initial condition at $t = 0$

$$P^{\mathrm{BF}}(\mathbf{E}0|\mathbf{E}_0 0) = W^{\mathrm{BF}}(\mathbf{E}_0)\delta(\mathbf{E} - \mathbf{E}_0) . \tag{C3}$$

The choice (C2) for $Q(E)$ guarantees that the stationary solution of (C1) (apart from an irrelevant multiplicative constant) indeed is $W^{\mathrm{BF}}(E) W^{\mathrm{BF}}(E_0)$. Equation (C1) can be solved by means of Laplace transformation. If we define

$$\tilde{P}^{\mathrm{BF}}(\mathbf{E}, \mathbf{E}_0; s) = \int_0^{\infty} dt\, P^{\mathrm{BF}}(\mathbf{E}t|\mathbf{E}_0 0) \exp(-st) \tag{C4}$$

and take into account the initial condition (C3), the Laplace transformation of (C1) leads to

$$\tilde{P}^{\mathrm{BF}}(\mathbf{E}, \mathbf{E}_0; s) = \frac{W^{\mathrm{BF}}(E_0)}{s + \nu(E)} \delta(\mathbf{E} - \mathbf{E}_0) + \frac{\tilde{R}(\mathbf{E}_0; s) Q(E)}{s + \nu(E)} , \tag{C5}$$

with

$$\tilde{R}(\mathbf{E}_0; s) = \int d\mathbf{E}\, \nu(E) \tilde{P}^{\mathrm{BF}}(\mathbf{E}, \mathbf{E}_0; s) . \tag{C6}$$

The multiplication of each side of (C5) by $\nu(E)$ followed by an integration over $\mathbf{E}$ provides a self-consistent equation for $\tilde{R}(\mathbf{E}_0; s)$, the solution of which is

$$\tilde{R}(\mathbf{E}_0; s) = \frac{\nu(E_0) W^{\mathrm{BF}}(E_0)}{[s + \nu(E_0)] \left[1 - \frac{1}{\langle \nu \rangle^{\mathrm{BF}}} \left\langle \frac{\nu^2}{(s+\nu)} \right\rangle^{\mathrm{BF}} \right]} , \tag{C7}$$

with

$$\begin{aligned} \langle \nu \rangle^{\mathrm{BF}} &= \int d\mathbf{E}\, \nu(E) W^{\mathrm{BF}}(E) , \\ \left\langle \frac{\nu^2}{(s+\nu)} \right\rangle^{\mathrm{BF}} &= \int d\mathbf{E} \frac{\nu^2(E)}{s + \nu(E)} W^{\mathrm{BF}}(E) . \end{aligned} \tag{C8}$$

Replacing $\tilde{R}(\mathbf{E}_0; s)$ by (C7) in (C5) we finally obtain

$$\tilde{P}^{\mathrm{BF}}(\mathbf{E},\mathbf{E}_0;s)=\frac{W^{\mathrm{BF}}(E_0)}{s+\nu(E)}\delta(\mathbf{E}-\mathbf{E}_0)+\frac{\nu(E)\nu(E_0)W^{\mathrm{BF}}(E)W^{\mathrm{BF}}(E_0)}{\left[\langle\nu\rangle^{\mathrm{BF}}-\left\langle\frac{\nu^2}{(s+\nu)}\right\rangle^{\mathrm{BF}}\right][s+\nu(E)][s+\nu(E_0)]} . \tag{C9}$$

In order to find a simple closed analytic expression for $P^{\mathrm{BF}}(\mathbf{E}t|\mathbf{E}_0 0)$, we make the approximation $\langle\nu^2/(s+\nu)\rangle^{\mathrm{BF}}=(\langle\nu\rangle^{\mathrm{BF}})^2/(s+\langle\nu\rangle^{\mathrm{BF}})$ [the latter is an identity in the Poisson-step process where $\nu(E)$ is constant]. The second term in the rhs of (C9) then becomes a rational fraction in s which is the Laplace transform of a linear combination of exponentials in t. The corresponding expression for $P^{\mathrm{BF}}(\mathbf{E}t|\mathbf{E}_0 0)$ is

$$P^{\mathrm{BF}}(\mathbf{E}t|\mathbf{E}_0 0)=W^{\mathrm{BF}}(E_0)\exp[-\nu(E_0)t]\delta(\mathbf{E}-\mathbf{E}_0)+W^{\mathrm{BF}}(E)W^{\mathrm{BF}}(E_0)\left[1-\frac{\nu(E_0)[\nu(E)-\langle\nu\rangle^{\mathrm{BF}}]}{\langle\nu\rangle^{\mathrm{BF}}[\nu(E)-\nu(E_0)]}\exp[-\nu(E)t]-\frac{\nu(E)[\nu(E_0)-\langle\nu\rangle^{\mathrm{BF}}]}{\langle\nu\rangle^{\mathrm{BF}}[\nu(E_0)-\nu(E)]}\exp[-\nu(E_0)t]\right] . \tag{C10}$$

The Fourier transformation of (C10) with respect to $\mathbf{E}$ and $\mathbf{E}_0$ leads to the expression (4.18) for A_t^{BF} with $P^{\mathrm{BF}}(E)=4\pi E^2 W^{\mathrm{BF}}(E)$.

The covariance $\Gamma^{\mathrm{BF}}(t)$ can be directly computed from (C1) without explicitly solving this equation for $P^{\mathrm{BF}}(\mathbf{E}t|\mathbf{E}_0 0)$. Indeed, if we multiply each side of (C1) by $\mathbf{E}\cdot\mathbf{E}_0$ and integrate the resulting equality over $\mathbf{E}_0$, we obtain

$$\frac{\partial}{\partial t}\int d\mathbf{E}_0\mathbf{E}\cdot\mathbf{E}_0 P^{\mathrm{BF}}(\mathbf{E}t|\mathbf{E}_0 0)=-\nu(E)\int d\mathbf{E}_0\mathbf{E}\cdot\mathbf{E}_0 P^{\mathrm{BF}}(\mathbf{E}t|\mathbf{E}_0 0) , \tag{C11}$$

where we have used that $\int d\mathbf{E}'\nu(E')P^{\mathrm{BF}}(\mathbf{E}'t|\mathbf{E}_0 0)$ only depends on the modulus E_0 (and on t of course). Taking into account the initial condition

$$\int d\mathbf{E}_0\mathbf{E}\cdot\mathbf{E}_0 P^{\mathrm{BF}}(\mathbf{E}0|\mathbf{E}_0 0)=E^2 W^{\mathrm{BF}}(E) , \tag{C12}$$

which follows from (C2), we easily integrate the linear ordinary differential equation (C11) as

$$\int d\mathbf{E}_0\mathbf{E}\cdot\mathbf{E}_0 P^{\mathrm{BF}}(\mathbf{E}t|\mathbf{E}_0 0)=E^2 W^{\mathrm{BF}}(E)\exp[-\nu(E)t] . \tag{C13}$$

We then infer

$$\Gamma^{\mathrm{BF}}(t)=\int d\mathbf{E}\,E^2 W^{\mathrm{BF}}(E)\exp[-\nu(E)t] . \tag{C14}$$

Let us determine a function $\nu(E)$ which corresponds to the choice (4.11) of $\Gamma^{\mathrm{BF}}(t)$. Assuming *a priori* that $\nu(E)$ is monotonic, we can rewrite (C14) as

$$\Gamma^{\mathrm{BF}}(t)=\int_{\nu(0)}^{\infty}d\nu\frac{dE(\nu)}{d\nu}E^2(\nu)P^{\mathrm{BF}}(E(\nu))\exp(-\nu t) , \tag{C15}$$

where $E(\nu)$ is the inverse function of $\nu(E)$ [$\nu(E(\nu))=\nu$]. We see that (C15) does reduce to (4.11) if we impose

$$\frac{d\nu(E)}{dE}=\frac{E^2 P^{\mathrm{BF}}(E)}{4e^2\rho(2\pi\beta m)^{1/2}} , \tag{C16}$$

$$\nu(0)=-\left[\frac{2\pi}{3}\right]^{1/2}\frac{u_{\mathrm{exc}}(\Gamma)}{\Gamma^{3/2}}\omega_p . \tag{C17}$$

The integration of the ordinary differential equation (C16) with the initial condition (C17) leads to the expression (4.12) for $\nu(E)$. This expression is indeed monotonic and always positive. When $E\to\infty$, $\nu(E)$ diverges: this behavior is compatible with the physical fact that large fields are produced by charges close to the considered radiator and consequently vary rapidly in time.

APPENDIX D

In this appendix, we derive the exponentiated-response form (4.15) of $H(l)$. Our starting point is the exact expression (2.26) for $H(l)$. Using a coupling-parameter integration technique, we rewrite the latter as

$$H(l)=\exp\left[-\frac{1}{2m\beta}\int_0^{l^2}d\lambda\int d\mathbf{r}\,\rho g_\lambda(\mathbf{r})\varphi(\mathbf{r})\right] , \tag{D1}$$

with

$$\varphi(\mathbf{r})=\frac{e^2}{r^6}\left[1+\frac{3x^2}{r^2}\right] \tag{D2}$$

and $\rho g_\lambda(\mathbf{r})$ is the one-body density of the particles submitted to the external potential $\lambda\varphi(\mathbf{r})/(2m\beta^2)$ created by a fictitious scatterer fixed at the origin. For a system of free particles, $g_\lambda(\mathbf{r})$ reduces to $\exp[-\lambda\varphi(\mathbf{r})/(2m\beta)]$ and then one easily finds from (D1) the free expression (4.14) of $H(l)$. For the present system of interacting particles, we shall introduce an approximate form of $g_\lambda(\mathbf{r})$ which interpolates between exact results at small and large distances and takes into account a neutrality constraint.

The small-distance behavior of $g_\lambda(\mathbf{r})$ can be obtained from

$$\rho g_\lambda(\mathbf{r})=\frac{N\exp\left[-\frac{\lambda\varphi(\mathbf{r})}{2m\beta}\right]\int d\mathbf{r}_2\cdots d\mathbf{r}_N\exp\left[-\beta V(\mathbf{r},\mathbf{r}_2,\ldots,\mathbf{r}_N)-\frac{\lambda}{2m\beta}\sum_{j=2}^{N}\varphi(\mathbf{r}_j)\right]}{\int d\mathbf{r}_1\cdots d\mathbf{r}_N\exp\left[-\beta V(\mathbf{r}_1,\ldots,\mathbf{r}_N)-\frac{\lambda}{2m\beta}\sum_{j=1}^{N}\varphi(\mathbf{r}_j)\right]} \tag{D3}$$

by expanding $V(\mathbf{r},\mathbf{r}_2,..,\mathbf{r}_N)$ in Taylor series around $V(\mathbf{0},\mathbf{r}_2,\ldots,\mathbf{r}_N)$. This gives

$$g_\lambda(\mathbf{r})\sim\text{const}\times\exp\left[-\frac{\lambda\varphi(\mathbf{r})}{2m\beta}\right],\quad r\to 0\ . \tag{D4}$$

For studying the large-distance behavior of $g_\lambda(\mathbf{r})$, we use the perturbative expansion of $[g_\lambda(\mathbf{r})-1]$ in powers of $\lambda\varphi(\mathbf{r})/(2m\beta^2)$,

$$g_\lambda(\mathbf{r})-1=-\frac{\lambda}{2m\beta}\int d\mathbf{r}' S(|\mathbf{r}'-\mathbf{r}|)\varphi(\mathbf{r}')+O(\lambda^2)\ . \tag{D5}$$

Strictly speaking, the integral in the rhs of (D5) as well as all the other spatial integrals involved in the expansion diverge because the singularity of $\varphi(\mathbf{r}')$ at the origin is nonintegrable. However, these term-by-term divergent contributions can be resummed into a finite one involving the Mayer function $\exp[-\lambda\varphi(\mathbf{r})/(2m\beta)]-1$. Taking into account the exponential decay of all the intrinsic particle correlations of the system (at $\lambda=0$), the latter contribution also decays exponentially when $r\to\infty$. Since $\varphi(\mathbf{r}')$ decays algebraically when $r'\to\infty$, the region $\mathbf{r}'$ close to $\mathbf{r}$ in the integral in (D5) gives algebraic contributions to $[g_\lambda(\mathbf{r})-1]$. Expanding $\varphi(\mathbf{r}')$ in Taylor series around $\varphi(\mathbf{r})$, we obtain

$$\begin{aligned} g_\lambda(\mathbf{r})-1&\sim\frac{\lambda}{8\pi m\beta^2e^2\rho}\nabla^2\varphi(\mathbf{r})\\ &=\frac{9\lambda}{2\pi m\beta^2\rho r^8}\left[1+\frac{2x^2}{r^2}\right],\quad r\to\infty \end{aligned} \tag{D6}$$

where we have used the charge, dipole and Stillinger-Lovett second-moment sum rules for $S(|\mathbf{r}'-\mathbf{r}|)$,

$$\begin{aligned} &\int d\mathbf{r}' S(|\mathbf{r}'-\mathbf{r}|)=0\ ,\\ &\int d\mathbf{r}'(\mathbf{r}'-\mathbf{r})S(|\mathbf{r}'-\mathbf{r}|)=\mathbf{0}\ ,\\ &\int d\mathbf{r}'(\mathbf{r}'-\mathbf{r})^2S(|\mathbf{r}'-\mathbf{r}|)=\frac{-3}{2\pi\beta e^2\rho} \end{aligned} \tag{D7}$$

(these sum rules are reviewed by Martin[21]). The terms $O(\lambda^2)$ in (D5) also give algebraic contributions to $[g_\lambda(\mathbf{r})-1]$, but the latter decay faster than the leading contribution (D6) of the linear term. The lack of exponential clustering for $g_\lambda(\mathbf{r})$ is due to the non-Coulombic nature of the external potential $\lambda\varphi(\mathbf{r})/(2m\beta^2)$ and is linked to the algebraic nature of the dynamical screening (see Ref. 30). Finally, we have the overall neutrality sum rule

$$\int d\mathbf{r}[g_\lambda(\mathbf{r})-1]=0 \tag{D8}$$

valid for any value of λ. This sum rule, which holds for a wide class of localized inhomogeneities (see, for instance, Ref. 21), can be inferred from the first Born-Green-Yvon (BGY) equation combined with clustering assumptions which are indeed satisfied here.

The exact behaviors (D4) and (D6) together with the sum rule (D8) provide constraints for the choice of the approximate $g_\lambda(\mathbf{r})$. We set

$$g_\lambda^{\mathrm{ER}}(r)=\exp\left\{-\frac{\lambda e^2}{2m\beta r^6}+C_\lambda\left[1-\exp\left[-\frac{\lambda e^2}{2C_\lambda m\beta r^6}-\frac{6\lambda a^3}{C_\lambda m\beta^2 r^8}\right]\right]\right\}, \tag{D9}$$

where the constant C_λ is determined by imposing $g_\lambda^{\mathrm{ER}}(r)$ to satisfy the neutrality constraint (D8). This simplified isotropic form of $g_\lambda(\mathbf{r})$ does behave as the isotropic terms (which do not depend on x) in the asymptotic behaviors (D4) and (D6). In order to take into account anisotropic effects, we replace the spatial integral in (D1) by

$$\frac{3e^2}{a^3}\left[1+\frac{\operatorname{arg\,sinh}\sqrt{3}}{2\sqrt{3}}\right]\int_0^\infty dr\frac{1}{r^4}g_\lambda^{\mathrm{ER}}(r)\ , \tag{D10}$$

where the coefficient $[1+(\operatorname{arg\,sinh}\sqrt{3})/(2\sqrt{3})]$ is the ratio of the corresponding integrals evaluated with the free expressions associated to external potentials $\lambda\varphi(\mathbf{r})/(2m\beta^2)$ and $\lambda e^2/(2m\beta^2r^6)$, respectively. This finally leads to the expression (4.15) for $H^{\mathrm{ER}}(l)$.

*Present address: Laboratoire de Physique de l'Ecole Normale Supérieure de Lyon, 46 allée d'Italie, 69364 Lyon CEDEX 07, France.

[1]See, e.g., H. R. Griem, *Spectral Line Broadening by Plasmas* (Academic, New York, 1974).

[2]A. Brissaud and U. Frisch, J. Quant. Spectrosc. Radiat. Transfer **11**, 1767 (1971).

[3]W. R. Chappel, J. Cooper and E. W. Smith, J. Quant. Spectrosc. Radiat. Transfer **9**, 149 (1969).

[4]See, e.g., J. W. Dufty, in *Strongly Coupled Plasma Physics,* edited by F. J. Rogers and H. E. DeWitt (Plenum, New York, 1987); S. Ichimaru, H. Iyetomi, and S. Tanaka, Phys. Rep. **149**, 91 (1987).

[5]J. Holtsmark, Ann. Phys. (Leipzig) **58**, 577 (1919).

[6]J. Seidel, Z. Naturforsch. A **32**, 1195 (1977).

[7]J. Seidel, Z. Naturforsch. A **34**, 1385 (1979).

[8]E. W. Smith, B. Talin and J. Cooper, J. Quant. Spectrosc. Radiat. Transfer **26**, 229 (1981).

[9]C. A. Iglesias, Phys. Rev. A **27**, 2705 (1983).

[10]C. A. Iglesias, J. L. Lebowitz, and D. MacGowan, Phys. Rev. A **28**, 1667 (1983).

[11]A. Alastuey, C. A. Iglesias, J. L. Lebowitz, and D. Levesque, Phys. Rev. A **30**, 2537 (1984).

[12]The autocorrelation function of the electric microfield "seen" by a moving ion has been studied by D. B. Boercker, J. W. Dufty, and C. A. Iglesias, Phys. Rev. A **36**, 2254 (1987). These

authors also propose a unified description of the radiative and transport properties of such an ion, which is in good agreement with computer simulation data, as confirmed by D. B. Boercker, in *Spectral Line Shapes* (Ossolineum, Wroclaw, 1989), Vol. 5.

[13]Strictly speaking, the fundamental ingredients of these short-time expansions are the conditional moments introduced by S. Chandrasekhar and J. von Neumann, Astrophys. J. **95**, 489 (1942), as shown by V. I. Kogan, in *Plasma Physics and the Problems of Controlled Thermonuclear Reactions,* edited by M. A. Leontovich (Pergamon, Oxford, 1960), Vol. IV. These moments are the equilibrium averages of the squares of the longitudinal and transverse [with respect to $\mathcal{E}(t)$] components of $d\mathcal{E}/dt$, calculated with the restriction $\mathcal{E}(t)=\mathbf{E}$.

[14]The mathematical proofs of the existence of the thermodynamic limit for the thermodynamic functions and the particle correlations in Coulomb systems are reviewed, respectively, by E. H. Lieb, Rev. Mod. Phys. **48**, 553 (1976), and D. Brydges and P. Federbush, in *Rigorous Atomic and Molecular Physics,* edited by G. Velo and A. S. Wightman (Plenum, New York, 1981).

[15]J. B. Taylor, Phys. Fluids **3**, 792 (1960).

[16]J. W. Dufty, D. B. Boercker, and C. A. Iglesias, Phys. Rev. A **31**, 1681 (1985) have shown that the effective-field representation of $W(E)$ corresponds to the first term of a renormalized Baranger-Mozer series. Their formalism provides the first corrections to this approximation in a systematic way, for any choice of the static effective field.

[17]The "three-pole" approximation for ordinary liquids was first proposed by S. W. Lovesey, J. Phys. C **4**, 3057 (1971). It has been extended to the OCP and compared to MD data by M. C. Abramo and M. Parrinello, Lett. Nuovo Cimento **12**, 667 (1975).

[18]See, e.g., J. P. Hansen and I. R. McDonald, *Theory of Simple Liquids,* 2nd ed. (Academic, London, 1986).

[19]For instance, we have used the HNC form of $\tilde{S}(k)$ which is quite good in the intermediate coupling regime. The existing approximations for $\tilde{S}(k)$ are described in the review on the static properties of the OCP by A. Alastuey, Ann. Phys. (Paris) **11**, 653 (1986).

[20]M. Baus and J. P. Hansen, Phys. Rep. **59**, 1 (1980).

[21]Ph. A. Martin, Rev. Mod. Phys. **60**, 1075 (1988).

[22]J. P. Hansen, I. R. McDonald, and E. L. Pollock, Phys. Rev. A **11**, 1025 (1975).

[23]R. Balescu, *Equilibrium and Non-equilibrium Statistical Mechanics* (Wiley-Interscience, New York, 1975); P. Vieillefosse and J. P. Hansen, Phys. Rev. A **12**, 1106 (1975).

[24]J. P. Hansen, Phys. Rev. A **8**, 3096 (1973).

[25]J. P. Hansen and I. R. McDonald, Phys. Rev. A **23**, 2041 (1981).

[26]S. W. de Leeuw, J. W. Perram, and E. R. Smith, Proc. R. Soc. London Ser. A **373**, 27 (1980).

[27]W. L. Slattery, G. D. Doolen, and H. E. DeWitt, Phys. Rev. A **26**, 2255 (1982).

[28]The first zero of $\Gamma(t)$ is well approximated by the smaller root of the polynomial corresponding to the first three terms of the small-time expansion (2.18). The parameter η_A could then be determined by imposing the first zero of $\Gamma^{\mathrm{AP}}(t)$ to be this root which only depends on $u_{\mathrm{exc}}(\Gamma)$ (we have checked that this simplification does not affect significantly the overall accuracy of APEX).

[29]The fit of χ_T^0/χ_T is obtained by differentiation with respect to Γ of the fit of $u_{\mathrm{exc}}(\Gamma)$, as described in Ref. 20.

[30]We stress that the dynamical screening is not exponential like the static one, as argued by A. Alastuey and Ph. A. Martin, Europhys. Lett. **6**, 385 (1988), who give strong evidences for an algebraic decay of $S(r,t)$ at $t\neq 0$. Consequently the effective field $\mathbf{e}_t^*(\mathbf{r})$ has to decay as an inverse power law when $r\to\infty$ for $t\neq 0$ [this behavior is indeed displayed by the APEX field $\mathbf{e}_t^{\mathrm{AP}}(\mathbf{r})$ used in this paper].

[31]J. W. Dufty and L. Zogaib, in *Strongly Coupled Plasma Physics,* edited by S. Ichimaru (Elsevier, Amsterdam, 1990).

[32]E. L. Pollock and J. C. Weisheit, in *Spectral Line Shapes III,* edited by R. Rostas (de Gruyter, New York, 1985), have studied a simplified version of the Brissaud-Frisch theory which amounts to replace the jumping time density $\nu(E)$ by a constant ν. These authors test the predictions of the theory against MD data, for frequency profiles computed from the scalar and magnitude models.